

JGR Solid Earth

RESEARCH ARTICLE

10.1029/2024JB029136

Key Points:

- We test whether continents can trigger subduction initiation on the early Earth using convection models with graindamage
- Model results show continents do not necessarily lead to subduction initiation, imparting only a minor increase in lithospheric stress
- Scaling analysis shows that continents are not capable of triggering subduction on the early Earth

Supporting Information:

Supporting Information may be found in the online version of this article.

Correspondence to:

H. Choi, hxc5400@psu.edu

Citation:

Choi, H., & Foley, B. J. (2024). A limited effect of continents on subduction initiation for convection with grain-damage. *Journal of Geophysical Research:* Solid Earth, 129, e2024JB029136. https://doi.org/10.1029/2024JB029136

Received 28 FEB 2024 Accepted 11 SEP 2024

Author Contributions:

Writing – original draft: H. Choi Writing – review & editing: B. J. Foley

© 2024. The Author(s). This is an open access article under the terms of the Creative Commons Attribution License, which permits use, distribution and reproduction in any medium, provided the original work is properly cited.

A Limited Effect of Continents on Subduction Initiation for Convection With Grain-Damage

H. Choi¹ and B. J. Foley¹

¹Department of Geosciences, Pennsylvania State University, University Park, PA, USA

Abstract Despite significant study, when and how plate tectonics initiated on Earth remains contentious. Geologic evidence from some of Earth's earliest cratons has been interpreted as reflecting the formation of initial continental blocks by non-subduction processes, which then trigger subduction initiation at their margins. Numerical models of mantle convection with a plastic yield stress rheology have shown this scenario is plausible. However, whether continents can trigger subduction initiation has not been tested with other rheologies. We, therefore, use numerical models of mantle convection with an imposed continental block to test whether continents facilitate subduction initiation with a grain-damage mechanism, where weak shear zones form by grain size reduction. Our results show that continents modestly enhance stresses in the lithosphere, but not enough to significantly impact lithospheric damage or subduction initiation: continents have minimal influence on lithospheric damage or plate speed, nor does subduction preferentially initiate at the continental margin. A new regime diagram that includes continental blocks shows only a small shift in the boundary between the mobile-lid and stagnant-lid regimes when continents are added. However, as we do find that stresses are modestly enhanced at the continental margin in our models, we develop a scaling law for this stress enhancement to more fully test whether continents could trigger subduction initiation on early Earth. We find that lithospheric stresses supplied by continents are not sufficient to initiate subduction on the early Earth on their own with grain-damage rheology; instead, additional factors would be required.

Plain Language Summary How plate tectonics initiates on Earth is controversial. One possibility is that primitive continents trigger subduction initiation at their margins; an idea our study tests with computer models. We specifically use a mechanism called grain-damage in our model, where weak zones that allow for subduction develop due to grain size reduction. The results showed only modest effects on lithospheric damage from the addition of continents. Continents do not appear to dictate the subduction initiation location, as subduction initiates readily both at continent margins and far from margins. In addition, plate boundaries do not get weaker nor do plates move faster with continents included. We observe slightly higher stress at continental margins, which leads to plate tectonics developing for a few models where it otherwise would not have. However, scaling our results to early Earth conditions, we find continents do not impart enough stress in the lithosphere on their own for subduction to initiate by grain size reduction. Other factors may have been important during this critical phase in our planet's history.

1. Introduction

1.1. Plate Tectonics Initiation

Plate tectonics is the major driver of physical and chemical processes on the modern Earth, controlling the location of earthquakes, volcanoes, and mountain ranges and shaping the structure and composition of the crust. The importance of plate tectonics extends beyond these geophysical and geochemical features of Earth, however, as it is thought to even play a key role in establishing a stable climate and surface conditions conducive to life. Plate tectonics drives uplift and orogeny, which are critical for chemical weathering to operate and stabilize Earth's climate (Foley, 2015; Kasting & Catling, 2003; Maher & Chamberlain, 2014). Plate tectonics may also have been a key factor in the origin of life on Earth by providing environments favorable for prebiotic chemistry at hydrothermal vents or subaerial continents (Bada & Korenaga, 2018; Dick, 2019; Martin et al., 2008; Parnell, 2004; Santosh et al., 2017) However, despite its importance, when and how plate tectonics began is poorly constrained (e.g., Cawood et al., 2006; Condie & Kröner, 2008; Korenaga, 2013; Stern & Gerya, 2018), mainly due to the scarcity of the rock record on early Earth and difficulty in uniquely interpreting this record in terms of global tectonic processes.

CHOI AND FOLEY 1 of 25

Exemplifying the difficulty in constraining when plate tectonics began, plate tectonics onset times spanning a huge portion of Earth's history, from >4.0 Ga to ~1 Ga, have been suggested in previous studies based on interpretations of the ancient geologic record (Korenaga, 2013; Palin et al., 2020). Hopkins et al. (2008) argued for the initiation of plate tectonics in the Hadean based on studies of the Jack Hills zircons. Hopkins et al. (2008) inferred the formation conditions of the parent magma to the Jack Hills zircons as 700 °C and 7 kbar based on thermobarometry of inclusions in the zircons, and argued this magma generation setting lay along a geotherm consistent with subduction zones. On the other extreme, Stern (2005) suggested that plate tectonics did not start until blueschist and ultrahigh-pressure metamorphic rocks became widespread in the geologic record at ~1 Ga. However, the studies highlighted above represent the extreme end member onset times that have been proposed in the literature; the majority of geological studies argue for an onset time to plate tectonics during the Archean based on a number of geochemical and petrological indicators, such as the presence of ultrahigh-pressure terranes paired with ultrahigh-temperature granulite metamorphic belts, and Archean ophiolites resembling Neoproterozoic fore-arc ophiolites, formed in a suprasubduction zone setting that appear in the Archean (Brown, 2006; Cawood et al., 2006; Condie & Kröner, 2008; Van Kranendonk, 2011).

1.2. Possible Causal Relationship Between Continent Formation and Subduction Initiation

The continents are key for constraining early Earth tectonics as they provide the primary rock record that can be used to study early Earth tectonics. Moreover, some studies (discussed below) have argued the formation and growth of continents can feedback on geodynamic processes and potentially alter Earth's tectonic regime. Although much continental material is lost by surface erosion and subsequent sediment subduction, along with subduction erosion, some continental crust can endure for billions of years due to its buoyancy and the strength of underlying mantle roots. While the precise history of continental crust growth, especially during the Hadean and Archean, is controversial (e.g., Harrison, 2009), at least some felsic crust existed even in the Hadean as evidenced by the >4.0 Ga Jack Hills zircons and the ~4.0 Ga Acasta Gneiss Complex (AGC) (Bowring & Williams, 1999; lizuka et al., 2006). Therefore, continental crust provides a long record for studying early Earth tectonics. In addition to providing a long geologic record, continents themselves are created by the tectonic processes operating at their time of formation, providing a clear link between their geochemical characteristics and early Earth tectonics. In the modern Earth, continents are produced through partial melting at subduction zones caused by a release of fluids from the downgoing plate (Hawkesworth et al., 1977; Taylor & McLennan, 1981). However, the continental crust can also form via the burial and re-melting of hydrated mafic crust in a thick crustal pile, or "oceanic-plateau" setting (Bédard, 2018; Reimink et al., 2014; Van Kranendonk et al., 2015). To infer the crust formation processes active during the Hadean and Archean, much research has focused on the petrology and geochemistry of preserved continental crust. This work has provided valuable insights into the evolution of Earth's tectonic mode, from early stages to modern plate tectonics.

Beyond merely recording past tectonic processes on Earth, there is evidence that continents may trigger the initiation of subduction on the early Earth, and hence play an active role in the onset of plate tectonics. The rock record from the AGC, the oldest known extant rocks on Earth, has been interpreted to suggest that primitive continents acted as nuclei for the later initiation of subduction at their margins (Reimink et al., 2016). The oldest rocks in the AGC are characterized by low La/Yb ratios and high heavy rare-earth-element (HREE) patterns, indicating that they formed from the melting of a basaltic protolith at shallower depths than the classic tonalitetrondhjemite-granodiorite (TTG) rock suite that is typical of Archean continental crust (Reimink et al., 2016). Such rocks are considered "Icelandites," due to their similarity to felsic rocks formed in modern-day Iceland; if this geochemical similarity maps to a similar formation mechanism, then the earliest felsic rocks in the AGC formed in a plateau melting setting rather than a subduction setting. However, younger rocks in the AGC, formed at 3.6 Ga, are more akin to classic Archean TTGs, indicating deeper melting. Reimink et al. (2016) interpreted the progression from shallow melting to deeper melting as representing the formation of a continental nucleus through non-plate-tectonic processes, followed by the later initiation of subduction at this continental block's margin. Zircon Hf isotope data from Slave Basement Gneisses show a decreasing trend in ε Hf from \sim 4.0 – 3.55 Ga, followed by a jump to positive values at around 3.55 Ga (Reimink et al., 2019). This Hf isotope trend represents the formation of felsic crust from a long-lived mafic crustal source prior to 3.55 Ga, followed by melting of juvenile crust at 3.55 Ga, and Reimink et al. (2019) argues this pattern is consistent with a transition from plateau melting to subduction. Moreover, this same pattern of Hf isotope trends in zircons is seen globally as well during the same time period. Bauer et al. (2020) showed that zircons older than $\sim 3.8 - 3.6$ Ga show negative, decreasing

CHOI AND FOLEY 2 of 25

21699356, 2024, 10, Downloaded from https

/agupubs.onlinelibrary.wiley.com/doi/10.1029/2024JB029136, Wiley Online Library on [31/05/2025]. See the Terms and Conditions (https://onlinelibrary

.com/terms-and-conditions) on Wiley Online Library for rules of use; OA articles are governed by the applicable Creative Commons Licens

 ε Hf arrays, followed by a jump to 0 or positive ε Hf. They interpreted this trend as representing crust formation in a plateau melting, or heat-pipe setting (as in, e.g. Kemp, 2018; Moore & Webb, 2013) followed by a global transition to crust formation in a subduction setting from 3.8 to 3.6 Ga.

In addition to the geologic evidence for a link between continent formation and the initiation of subduction, such a link is also seen in some numerical geodynamic models as well. Rey et al. (2014) argued that gravitational spreading of rheologically weak Archean continents facilitate subduction initiation at their margin. This gravitational spreading leads to horizontal compression in the surrounding lithosphere, which is enough to overcome the lithospheric yield stress in their models and initiate subduction. Moreover, Rolf and Tackley (2011) further supports this idea by finding that mobile lid convection can persist at higher yield stress values with continents included than it can in models without continents. Finally, a global model that tracked sites of subduction initiation found that continental margins are preferred sites of subduction initiation, due to compressive stresses from the continents (Ulvrova et al., 2019).

However, all of these previous modeling studies used the pseudo-plastic yield stress rheology (Moresi & Solomatov, 1998). With the pseudoplastic rheology, the lithosphere is assumed to fail when an imposed yield stress is reached. Therefore, when stresses caused by mantle convection reach the yield stress, weak plate boundaries can form, and subduction initiates. Even though this approach can generate plate-like mantle convection, there are two major problems: (a) The yield stress value required for mobile lid convection to develop in most numerical models is approximately an order of magnitude lower (Moresi & Solomatov, 1998; Solomatov, 2004; Tackley, 2000a) than that suggested for Earth's lithosphere by lab experiments (Brace & Kohlstedt, 1980; Byerlee, 1978); (b) Pseudo-plasticity assumes the material recovers its strength immediately once the stress drops below the yield stress. Pre-existing weak zones, which are thought to be crucial for subduction initiation (Baes et al., 2011; Gurnis et al., 2004; Hall et al., 2003; McKenzie, 1977; Toth & Gurnis, 1998), cannot be explained with this mechanism. Therefore, we use a grain-damage mechanism in this study which generates plate boundaries through grain size reduction. This mechanism allows for weak zone memory and attempts to more completely represent the microphysical processes leading to lithospheric weakening (see Section 2.1 for a full description).

1.3. Purpose of the Study

The goal of this paper is therefore to test whether the formation of continental blocks can indeed trigger subduction initiation on the early Earth, as proposed by previous studies of early Earth geology and previous geodynamic studies. We perform this test by including chemically buoyant blocks representing continents in numerical models of mantle convection. We investigate the effects of several key parameters that can control subduction initiation: continental thickness, Rayleigh number, grain growth activation energy, which controls the damage-to-healing ratio in the lithosphere, and viscosity contrast between the continental block and surrounding mantle. We develop a scaling law for the stress enhancement due to the presence of a continent, and use this to estimate the amount of additional damage that continents can cause in the lithosphere during the Archean.

2. Methods

2.1. Grain-Damage Mechanism for Plate Boundary Formation

Grain-damage is the theoretical formulation for proposed feedback between deformation-induced grain size reduction and grain size-dependent viscosity: deformation causes grain size reduction in the lithosphere, which leads to rheological weakening through the grain size dependent viscosity, additional focusing of deformation in the forming shear zone, and so on (Bercovici & Ricard, 2012; Bercovici et al., 2001). Such feedback between grain size reduction and grain size sensitive flow was initially thought to be problematic based on monominerallic rheology experiments. Grain size reduction through dynamic recrystallization occurs predominantly via dislocation creep, while grain size-sensitive flow occurs in diffusion creep or grain boundary sliding regimes. These regimes sit in distinct grain size, stress, temperature, and pressure spaces, and thus may not be able to interact in a positive feedback (De Bresser et al., 2001). Without the co-existence of grain size sensitive flow and grain size reduction, grain size would be driven to the "field" boundary between dislocation creep and diffusion creep or grain boundary sliding, leading to minimal rheological weakening. However, in polymineralic rocks (rocks made up of multiple mineral phases) damage can occur to the interface between mineral phases regardless of the dominant creep mechanism, and damage to the phase interface ultimately leads to grain size reduction to co-exist,

CHOI AND FOLEY 3 of 25

21699356, 2024, 10, Downloaded from https

ibrary.wiley.com/doi/10.1029/2024JB029136, Wiley Online Library on [31/05/2025]. See the Terms

and hence act as a positive feedback mechanism to create weak, localized shear zones (Bercovici & Ricard, 2012, 2013). Natural shear zones show evidence of significant rheological weakening occurring through grain size reduction (Skemer & Karato, 2008; Warren & Hirth, 2006), as the grain damage mechanism relies on. Moreover, recent laboratory experiments with polymineralic samples show grain size reduction and rheological weakening continuing in the diffusion creep regime (Bercovici et al., 2023; Cross & Skemer, 2019; Tasaka et al., 2017; Wiesman et al., 2018), as Bercovici and Ricard (2012) proposed.

We assume the mantle in our models can be represented by peridotite, a polymineralic mixture of olivine and pyroxene minerals. We use the grain-damage theory from Bercovici and Ricard (2012), which provides a grain size evolution equation for both mineral phases and an equation for the "roughness" of the phase interface. When the two phases are well mixed together, a "pinned state" is reached, where the phase interface roughness determines the grain size of both mineral phases. In the pinned state, the grain size evolution of either phase can be solved for directly through an equation that follows the same form as the interface roughness equation, as interface roughness is ultimately controlling grain size (Bercovici & Ricard, 2012). The pinned state forms because Zener pinning of the secondary phase on the primary phase limits grain growth, and damage to the interface between phases leads to finer scale interface roughness, which increases the curvature of the mineral grains. Such increased curvature then drives grain size reduction to minimize surface energy, continuing until the mineral grain sizes scale with the interface roughness.

We assume that the pinned state prevails throughout our model domain, such that we only need to solve a single grain size evolution equation for the primary phase, olivine (Bercovici & Ricard, 2012; Foley, 2020; Foley & Rizo, 2017; Foley et al., 2014). We also assume diffusion creep is dominant throughout the mantle, and therefore, we do not include a composite rheology involving both diffusion and dislocation creep (Rozel et al., 2011). In reality, the rheology is controlled by whichever mechanism, dislocation or diffusion creep, allows for deformation the easiest. However, subduction initiation, the focus of this paper, occurs in lithospheric shear zones where damage drives grains to sizes low enough that dislocation creep is negligible. The rheology of the mantle interior, however, could be more strongly affected by neglecting dislocation creep. Our model results show, though, that the grain size of the interior mantle also remains small enough that neglecting dislocation creep does not significantly impact the results, even with high internal heating rates.

With the above assumptions, mantle viscosity is:

$$\mu = \mu_0 \exp\left(-\xi_{\nu} T\right) \left(\frac{A}{A_0}\right)^{-m} \tag{1}$$

where μ_0 is a constant, ξ_v describes the temperature-dependence of viscosity, A is the fineness or the inverse grain size, A_0 is a reference fineness, and m is the grain size sensitivity exponent; m = 2 is used in this study, consistent with Nabarro-Herring creep (Hirth & Kohlstedt, 2003). We use a linear exponential temperature-dependent viscosity rather than an Arrhenius formulation in this study to keep the number of free parameters to a minimum.

In the pinned state, the equation governing fineness evolution is given as:

$$\frac{DA}{Dt} = \frac{f}{\gamma} \Psi - hA^p \tag{2}$$

where t is time, f is the fraction of deformational work that goes into surface energy, thereby reducing grain size, γ is surface energy, Ψ is the rate of deformational work, h is the temperature-dependent healing rate, and p is the grain growth exponent; we use p=4 (Bercovici & Ricard, 2012). The first term of Equation 2's right-hand side represents grain size reduction. It states that a fraction, f, of the deformational work partitions into surface energy, therefore reducing grain size (and increasing fineness). The second term describes grain growth that releases surface energy stored on grain boundaries, modulated by the temperature-dependent healing rate, h. The healing rate is assumed to follow a linear-exponential form like viscosity, as

$$h = h_0 \exp(\xi_h T) \tag{3}$$

where h_0 is a constant and ξ_h describes the temperature dependence of grain growth.

CHOI AND FOLEY 4 of 25



Table 1		
Non-Dimensional	Model	Variables

Variable	Dimensional scaling factor	Definition	Reference equation
x'	d	Horizontal axis (x-axis)	_
t'	$\frac{d^2}{\kappa}$	Time	9 and 10
v'	$\frac{\kappa}{d}$	Velocity	7 and 9
T'	$\Delta T + T_s$	Temperature	8–10
A'	A_0	Fineness (inverse grain size)	10
C	C = 1 for continent, $C = 0$ for mantle	Composition	8
τ'	$rac{\mu_m \kappa}{d^2}$	Stress	-

The fraction of deformational work that partitions into surface energy, f, is not well constrained. Rough estimates of the ratio f/h, though, can be made by comparison to dynamic recrystallization experiments. However, in principle, dynamic recrystallization experiments provide a constraint on the partitioning of deformational work directly to the surface energy of the grains themselves; that is, damage to the grains directly. In the pinned state, though, it is damage to the interface between phases that then indirectly drives grain size reduction. The fraction of deformational work going toward damage to the phase interface could differ from that driving damage of the grains directly (Mulyukova & Bercovici, 2017). However, dynamic recrystallization experiments are currently the best available constraint, and given the similar physics between the two damage processes, should serve as a good proxy for interface damage. Comparisons of grain-damage theory to experiments find that for a low value of grain growth activation energy of 200 kJ/mol, f is likely temperature-dependent, decreasing with increasing temperature (Mulyukova & Bercovici, 2017; Rozel et al., 2011). However, as experiments only constrain f/h, f could instead be temperature-independent with grain growth featuring a larger activation energy. Foley (2018a) finds that, with an activation energy for grain growth of 430 kJ/mol, f is independent of temperature. Given this trade-off between temperature dependencies of f and h, we choose to keep f constant and assume all temperature dependence is contained in the grain growth rate, h.

2.2. Mantle Convection Modeling

We couple the above grain-damage formulation to standard Boussinesq convection. The equations for the conservation of mass, momentum, and energy are:

$$\nabla \cdot v = 0 \tag{4}$$

$$0 = -\nabla P + \nabla \cdot (2\mu \underline{\dot{\varepsilon}}) + \rho_0 g \alpha T - \Delta \rho_c C g \tag{5}$$

$$\frac{\partial T}{\partial t} + \underline{v} \cdot \nabla T = \kappa \nabla^2 T + \frac{Q_v}{\rho_0 c_p} \tag{6}$$

where v is velocity, P is the pressure, μ is viscosity, $\underline{\underline{\dot{e}}}$ is strain rate, ρ_0 is the average mantle density, g is gravity, κ is thermal diffusivity, $\Delta\rho_c$ is the density difference between the average mantle and continent due solely to their different chemical compositions, α is the thermal expansion coefficient, C represents chemical composition, c_p is the specific heat capacity at constant pressure, T is the temperature, t is time, and Q_v is the volumetric internal heating rate with a unit of W/m³. We further define $Q = \frac{Q_v}{\rho_0 c_p}$. The chemical component, C, corresponds to the continent when C = 1, and C = 0 corresponds to the mantle.

Using non-dimensional scaling factors (x = x'd); $t = \frac{t'd^2}{\kappa}$; $t = \frac{v'\kappa}{d}$; $t = T'\Delta T + T_s$; $t = A'A_0$; $t = \frac{Q'\kappa\Delta T}{d^2}$; $t = \frac{\tau'\mu_m\kappa}{d^2}$; where μ_m is the reference viscosity defined at $t = \Delta T + T_s$. (The full list of non-dimensional model variables and input parameters is in Tables 1 and 2), the above equations are rewritten in non-dimensionalized form, where primes indicate non-dimensional variables:

CHOI AND FOLEY 5 of 25

21699356, 2024, 10, Downloaded from https://agupubs.onlinelibrary.wiley.com/doi/10.1029/2024JB029136, Wiley Online Library on [31/05/2025]. See the Terms

Table 2
Non-Dimensional Input Parameters

Parameters	Definition	Assumed value	Reference equation
Ra_0	Reference Rayleigh number	10 ⁷	8
Ви	Buoyancy number	-1	8
D	Damage number	10^{-2}	10
H	Healing number	1.5×10^5	10
Q'	Internal heating rate	5 – 25	9
$ heta_{v}$	Frank-Kamenetskii parameter for viscosity	13.82	11 and 12
$ heta_h$	Frank-Kamenetskii parameter for healing	9.721 - 13.82	11

$$\nabla \cdot \underline{v}' = 0 \tag{7}$$

$$0 = -\nabla P' + \nabla \cdot \left(2\mu' \dot{\underline{\dot{\varepsilon}}}'\right) + Ra_0 \left(T' - Bu \cdot C\right) \hat{\underline{\zeta}}$$
 (8)

$$\frac{\partial T'}{\partial t'} + \underline{v}' \cdot \nabla T' = \nabla^2 T' + Q' \tag{9}$$

$$\frac{DA'}{Dt'} = D\Psi' \exp(\theta_{\nu}(1 - T'))A'^{-m} - H \exp(-\theta_{h}(1 - T'))A'^{p}$$

$$\tag{10}$$

where Ra_0 is the reference Rayleigh number $\left(Ra_0 = \frac{\rho_0 ag\Delta Td^3}{\kappa\mu_m}\right)$, where μ_m is a reference mantle viscosity defined at $T_m = \Delta T + T_s$ and $A = A_0$, $\Psi' = \frac{\dot{\varepsilon}}{\dot{\varepsilon}}' : \frac{\dot{\varepsilon}}{\dot{\varepsilon}}'$, and \hat{z} is the vertical unit vector. Buoyancy number, $Bu = \frac{\Delta\rho_c}{\rho_0 a\Delta T}$, is the ratio of density difference due to compositional changes over the density difference due to temperature changes. Our momentum equation is constructed such that a negative Bu value represents a material with a lower density than the reference mantle, while a positive Bu value represents a material with a higher density than the reference mantle. D is the non-dimensional damage number and D is the non-dimensional damage number and D is the non-dimensional healing number, defined as $D = \frac{f\mu_m\kappa}{\gamma A_0 d^2}$ and $D = \frac{h_m A_0^{(p-1)} d^2}{\kappa}$. The quantities D_0 and D_0 are the Frank-Kamenetskii parameters for viscosity and healing, which can be related to the activation energy, D_0 , from an Arrhenius law as:

$$\theta = \frac{E\Delta T}{R(T_c + \Delta T)^2} \tag{11}$$

where R is the universal gas constant. Using the activation energy for viscosity, E_v , in Equation 11, gives θ_v and using the activation energy for grain growth, E_h , gives θ_h . The non-dimensional viscosity is:

$$\mu' = \exp(\theta_{\nu} (1 - T')) A'^{-m} \tag{12}$$

2.3. Numerical Model Setup

The model domain is rectangular with a 4×1 aspect ratio and resolution of 512×128 , where horizontal and vertical grid spacing is equal. The models are purely internally heated, with an isothermal top boundary layer and no heat flux bottom boundary. Periodic boundary conditions are used for the left and right boundaries. The models were restarted from previously run mantle convection models (Foley, 2020), which had already reached thermal equilibrium in either mobile and stagnant-lid convection.

A rectangular continental block with thickness $d_{\rm cont}$ and length L is inserted into the models far from any plate boundaries, so that this continental block does not immediately interact with plate boundaries. A continental block in this study represents the continental crust and sub-continental lithospheric mantle as one unit. This is because

CHOI AND FOLEY 6 of 25

the crust itself is often too thin to be resolvable in our models. In this study, we explored a range of $d_{\rm cont} = 0.025 - 0.25$, which scales to 72.25 - 722.5 km. The thickness of deep continental lithospheric roots on modern Earth suggested from seismic tomography is 250–300 km (James et al., 2001), 160–220 km estimated from petrology (Boyd & Gurney, 1986; Griffin et al., 2003), and 160–300 km based on thermal models (Michaut et al., 2007). Our models therefore cover a range from thinner than typical continental lithosphere, to 2–2.5 times thicker, such that effect of continent thickness can be fully explored.

In addition to $d_{\rm cont}$, other key model parameters controlling the continental block in this study are Bu, L, and the ratio of continent viscosity to background mantle viscosity, $\mu_{\rm jump}$. Across all the simulations, Bu and L held fixed as -1 and 0.5, respectively, in the non-dimensional units. Assuming a sub-lithospheric upper mantle density of $\rho_{\rm um} = 3300 {\rm kg/m^3}$ (distinct from the average mantle density, $\rho_0 \approx 4000 {\rm kg/m^3}$), which includes contribution from higher densities of the deeper mantle, $\alpha = 3 \times 10^{-5} {\rm K^{-1}}$, and $\Delta T = 1350 {\rm K}$, Bu = -1 corresponds to $\Delta \rho_c = -134 {\rm kg/m^3}$. The compositional density difference of our modeled continental block is therefore consistent with the compositional density difference of continents on Earth, when both the crust and depleted mantle roots are averaged together. With typical estimates for the density and thickness of the continental crust as $\sim 2,800 {\rm kg/m^3}$ and $40 {\rm km}$, respectively, and $\sim 3,250 {\rm kg/m^3}$ and $200 {\rm km}$, respectively, for the depleted mantle lithosphere (Christensen & Mooney, 1995), the average density of continent that weighted by the thickness of both layers is $3,160 {\rm kg/m^3}$. Comparing this average to the typical density of the sub-lithospheric upper mantle of $3,300 {\rm kg/m^3}$, compositional density difference for continents on Earth is $\Delta \rho_c = -140 {\rm kg/m^3}$.

The sub-continental lithospheric mantle is thought to have a higher intrinsic viscosity than the ambient convecting mantle, as the lithospheric mantle has been depleted by partial melting and hence dehydrated (Pollack, 1986). Moreover, modeling studies have found that continental lithospheric roots need to have an elevated viscosity range of 100-1,000 times compared to the surrounding mantle so that they can resist entrainment and erosion by subduction for >2 Gyr timescales (Lenardic & Moresi, 1999; Manga & O'Connell, 1995). Consistent with this constraint for continent survival, we use $\mu_{\text{jump}} = 100$ in the convection models.

The internal heating rate, Q', varies from 5 to 25 in the numerical models. This range scales to $\approx 3-16$ TW, assuming d=2890 km, $\Delta T=1350$ K, $\kappa=10^{-6}$ m²/s, $\rho_0=4000$ kg/m³, and $c_p=10^3$ J/kg/K; lower than values expected for early Earth. However, we use relatively reduced values of internal heating rate so that our models produce internal temperatures within a reasonable range for the Archean Earth. Because we use weaker temperature-dependent viscosity and lower Ra than expected for the early Earth to keep the models numerically tractable, convective heat transfer is slower in our models. As a result, lower values of internal heating rate still produce warm mantle interior temperatures consistent with the early Earth.

We use a uniform $Ra_0 = 10^7$ for all models. Convective vigor is still effectively varied across the models, though, because varying Q' leads to different interior temperatures and, therefore, different effective internal Rayleigh numbers. Since the viscosity and healing are temperature dependent, the Frank-Kamenetskii parameters for viscosity (θ_v) and healing (θ_h) are required (See Equations 11 and 12). We use $\theta_v = 13.82$ for all models; this is lower than the typical value for diffusion creep (250–375 kJ/mol, from Fei et al. (2016); Hirth and Kohlstedt (2003)), but keeps the viscosity ratio between surface and interior at a numerically tractable 10^6 when T' = 1. The level of temperature-dependent viscosity variation in the models is more than enough to lead to stagnant-lid convection in the absence of grain-damage. Healing temperature dependence is not well constrained (Evans et al., 2001; Foley, 2018a; Mulyukova & Bercovici, 2017; Speciale et al., 2020), so we use a range of $\theta_h = 9.721-13.82$ to explore parameter space. Varying θ_h in our models is a way to control the healing rate in the lithosphere and, therefore, map the boundary between mobile-lid and stagnant-lid regimes (Foley, 2018b, 2020). $D = 10^{-2}$ and $D = 10^{-2}$ and $D = 10^{-2}$ are used for all models, which is within the range of estimates for Earth (Foley & Rizo, 2017).

3. Numerical Model Results

We use our numerical models to test whether including continents enhances lithospheric damage and promotes subduction initiation in three ways: (a) we test whether including continents expands the parameter space that allows for mobile lid convection; (b) whether subduction zones preferentially initiate at continental margins, due to enhanced lithospheric stresses from the continent; and (c) whether lithospheric damage in active shear zones and surface plate speeds are enhanced when continents are included or scale with continent thickness.

CHOI AND FOLEY 7 of 25

21699356, 2024, 10, Downloaded from https://agupubs.onlinelibrary.wiley.com/doi/10.1029/2024JB029136, Wiley Online Library on [31/05/2025]. See the Terms and Conditions (https://onlinelibrary.wiley.com/doi/10.1029/2024JB029136, Wiley Online Library on [31/05/2025]. See the Terms and Conditions (https://onlinelibrary.wiley.com/doi/10.1029/2024JB029136, Wiley Online Library on [31/05/2025]. See the Terms and Conditions (https://onlinelibrary.wiley.com/doi/10.1029/2024JB029136, Wiley Online Library on [31/05/2025]. See the Terms and Conditions (https://onlinelibrary.wiley.com/doi/10.1029/2024JB029136, Wiley Online Library.wiley.com/doi/10.1029/2024JB029136, Wiley Online Li

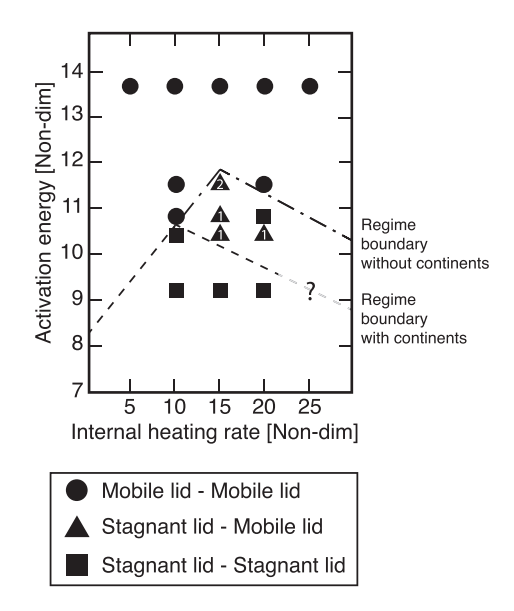


Figure 1. Regime diagram illustrating whether including continents changes the convection regime (stagnant lid or mobile lid) previously observed without continents. Each symbol represents the behavior seen in models over a range of continent thicknesses, as at each point in $Q' - \theta_h$ space models with a range of continent thicknesses were run. Triangles represent conditions where models showed a switch from a stagnant lid without continents to a mobile lid with continents, for at least one modeled value of continent thickness. The number inside the triangles indicates the number of models across the range of continent thicknesses tested where a regime switch is observed, as explained in more detail in the main text. The dot-dashed line represents the regime boundary observed without continents from Foley (2018b), and the new regime boundary with continents is illustrated with a dashed line.

We first develop a new regime diagram for the stagnant-lid and mobile-lid regimes in internal heating rate, Q', grain growth Frank-Kamenetskii parameter, θ_h , space, to test how continents of a range of thickness affect the regime boundary. The new regime diagram is directly comparable to those in Foley (2018b, 2020) without continents. Looking at regime boundary changes with continents included is important because it provides insight into the extent to which the presence of continents can cause a switch in the convection regime from stagnant lid to mobile lid. Such a regime switch in Figure 1 is defined as any continental thickness at given θ_h and Q' that results in a switch from a stagnant lid to a mobile lid state. If there is more than one model showing regime shifts with different $d_{\rm cont}$, it is considered as a single data point, marked as a triangle. The number inside of the triangle represents how many models with different $d_{\rm cont}$ show a regime shift from stagnant to mobile lid.

We find that most of our numerical models that include continents display the same convection regime as the models from Foley (2018b, 2020) regardless of the continental thickness; this encompasses models that lie far from the original, Foley (2018b) regime boundary in $Q' - \theta_h$ space. However, we do find that a few models near the original regime boundary shift from stagnantlid convection without continents to mobile-lid convection with continents, especially with Q' = 15 - 20. This regime shift is seen only when thick continental blocks are used. Specifically, when a regime shift is only seen for one model at a given Q' and θ_h , this occurs for the thickest continent case of $d_{\text{cont}} = 0.2$. For the Q' = 15, $\theta_h = 11.513$ case where two models show a regime shift, the regime switch is seen for the continent thickness of $d_{\rm cont} = 0.2$ and $d_{\rm cont} = 0.05$. The largest shift in the regime boundary occurs at Q' = 15, where the regime boundary without continents sat above $\theta_h = 11.513$, and with continents added lowers to $\theta_h \approx 10$. This difference in θ_h is equivalent to lowering the damage to healing ratio in the lithosphere, $D/(H \cdot h_l)$, by a factor of ≈ 5 .

Continents can drive a switch from stagnant-lid to mobile-lid convection due to their associated buoyancy forces. The buoyancy of continents induces a net upward buoyancy force, which, combined with the fixed upper boundary, causes the continent margins to push outwards against the surrounding lithosphere. Continents, therefore, induce horizontal compressive stresses as they attempt to gravitationally spread, resisted by the surrounding lithosphere. The net buoyancy force increases with increasing continent thickness, meaning thicker continents should cause higher stresses at their margins and therefore be more likely to induce subduction. That we only see a switch from stagnant-lid to mobile-lid regimes for thick continents supports this expectation that ticker continents can induce higher lithospheric stresses.

Another important role continents could play is influencing where new subduction zones initiate. As outlined in Section 1, some studies of early Earth geology suggest that the earliest formed continents could trigger subduction at their margins and act as nuclei for further continental growth. Moreover, convection models using a yield stress rheology find that continent margins are preferred sites for subduction initiation. Examining subduction initiation locations in our models can help test these ideas when the grain-damage mechanism is used. However, despite finding that adding continents can induce a switch from stagnant-lid to mobile-lid convection in limited cases, near the old regime boundary in $Q' - \theta_h$ space and for thick continents, results from the numerical models show that continents do not significantly affect subduction initiation locations. Figures 2 and 3 show images documenting the initiation of new subduction zones from two of the numerical models. They clearly show that subduction does not always start at the continental margins, but also initiates far from the continent margin (in these cases, between the continental margin and the existing subduction zone) and then slowly migrates toward the continental margin. Based on a similar visual inspection of the convection planform for all models, we see a mixture of some initiation at the margin and some far from the margins, with no preference for initiation at the continent margin.

CHOI AND FOLEY 8 of 25

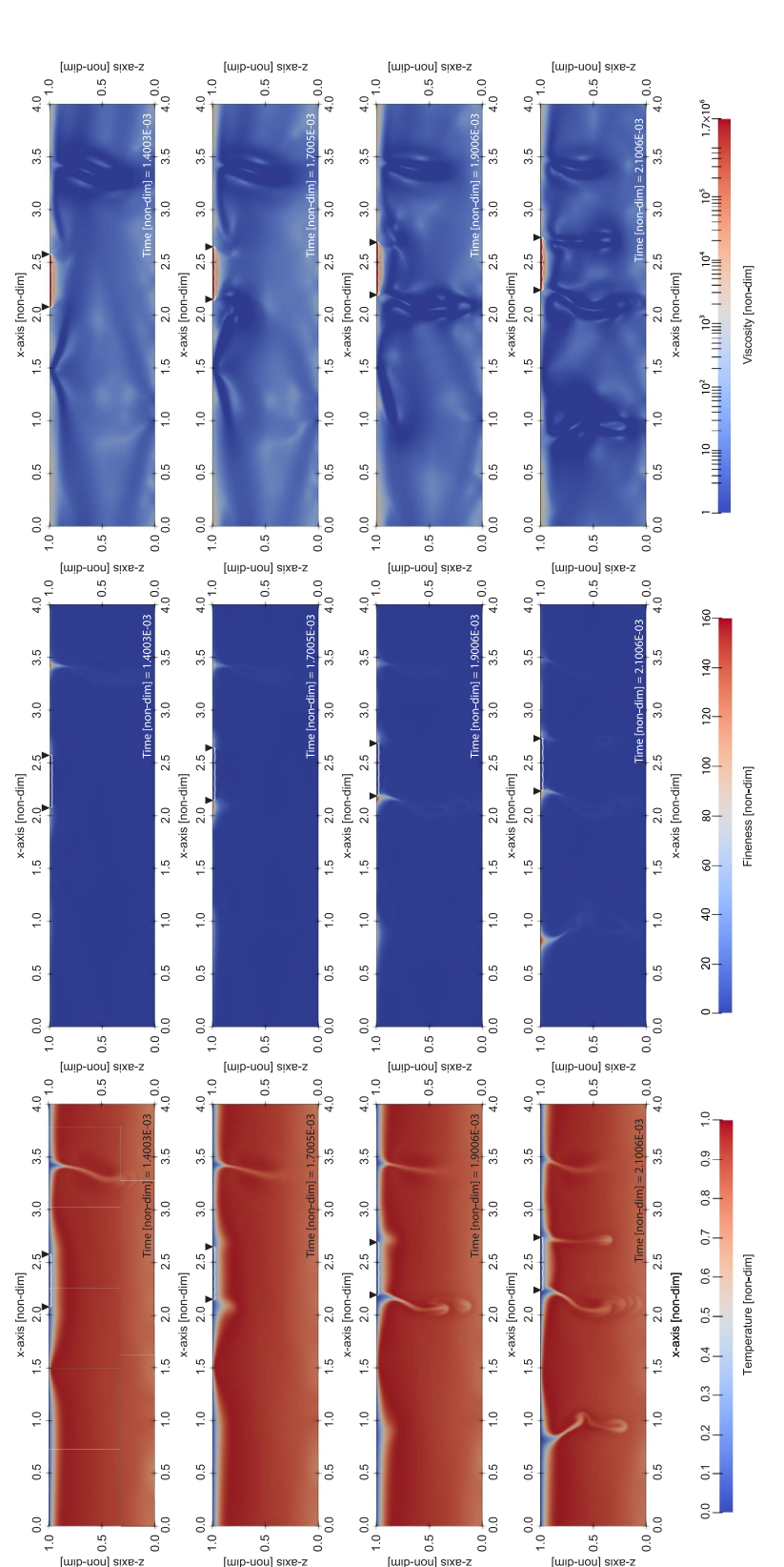


Figure 2. Snapshot of model with continental thickness $d_{cont} = 0.025$ over a non-dimensional timespan of 3×10^{-3} . The first column shows the evolution of the temperature, the second column shows the = 100. The outline of the continent is shown by a white line, another new subduction initiates around x' = 0.8, far from the continental margins. Over time, this subduction zone distant from continental margins slowly migrates toward a continental margin. $= 20, \theta_h = 13.82, \text{ and } \mu_{\text{lump}}$ and also the black triangles at the top surface mark the continent's locations. At time 1.7005×10^{-3} , the new subduction initiates around x'corresponding fineness field, and the third column shows the viscosity. Other parameters for this model are Q^\prime

21699356, 2024, 10, Downloaded from https://agupubs. onlinelibrary.wiley.com/doi/10.109/2024JB09136, Wiley Online Library on [31/05/2025]. See the Terms and Conditions (https://onlinelibrary.wiley.com/terms-and-conditions) on Wiley Online Library for rules of use; OA articles are governed by the applicable Creative Commons. Licensed Conditions (https://onlinelibrary.wiley.com/terms-and-conditions) on Wiley Online Library for rules of use; OA articles are governed by the applicable Creative Commons. Licensed Conditions (https://onlinelibrary.wiley.com/terms-and-conditions) on Wiley Online Library for rules of use; OA articles are governed by the applicable Creative Commons. Licensed Conditions (https://onlinelibrary.wiley.com/terms-and-conditions) on Wiley Online Library for rules of use; OA articles are governed by the applicable Creative Commons. Licensed Conditions (https://onlinelibrary.wiley.com/terms-and-conditions) on Wiley Online Library for rules of use; OA articles are governed by the applicable Creative Commons. Licensed Conditions (https://onlinelibrary.wiley.com/terms-and-conditions) on Wiley Online Library for rules of use; OA articles are governed by the applicable Creative Commons. Licensed Conditions (https://onlinelibrary.wiley.com/terms-and-conditions) on Wiley Online Library for rules of use; OA articles are governed by the applicable Creative Commons.

CHOI AND FOLEY 9 of 25

21699356, 2024, 10, Downloaded from https://agupubs. onlinelibrary.wiley.com/doi/10.109/2024JB09136, Wiley Online Library on [31/05/2025]. See the Terms and Conditions (https://onlinelibrary.wiley.com/terms-and-conditions) on Wiley Online Library for rules of use; OA articles are governed by the applicable Creative Commons. Licensed Conditions (https://onlinelibrary.wiley.com/terms-and-conditions) on Wiley Online Library for rules of use; OA articles are governed by the applicable Creative Commons. Licensed Conditions (https://onlinelibrary.wiley.com/terms-and-conditions) on Wiley Online Library for rules of use; OA articles are governed by the applicable Creative Commons. Licensed Conditions (https://onlinelibrary.wiley.com/terms-and-conditions) on Wiley Online Library for rules of use; OA articles are governed by the applicable Creative Commons. Licensed Conditions (https://onlinelibrary.wiley.com/terms-and-conditions) on Wiley Online Library for rules of use; OA articles are governed by the applicable Creative Commons. Licensed Conditions (https://onlinelibrary.wiley.com/terms-and-conditions) on Wiley Online Library for rules of use; OA articles are governed by the applicable Creative Commons. Licensed Conditions (https://onlinelibrary.wiley.com/terms-and-conditions) on Wiley Online Library for rules of use; OA articles are governed by the applicable Creative Commons.

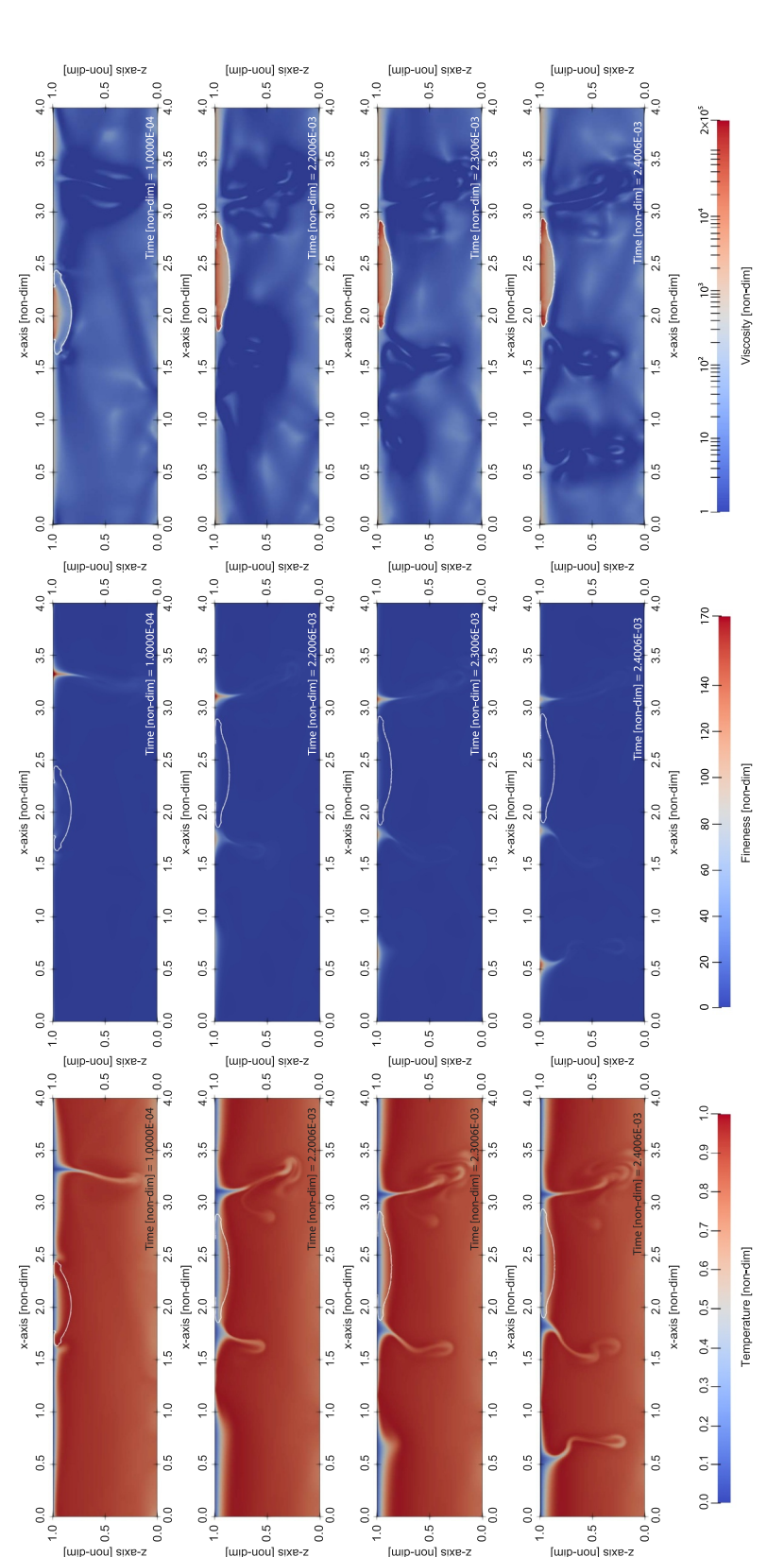


Figure 3. Model snapshots same as Figure 2, but now with $d_{cont} = 0.2$. At time 1.0000×10^{-4} , the new subduction initiates around x' = 1.5, near the left continental margin. At time 2.3006×10^{-3} , another new subduction initiates around x' = 0.6, but this time far from the continental margins.

CHOI AND FOLEY 10 of 25



Journal of Geophysical Research: Solid Earth

10.1029/2024JB029136

In addition, we also see a consistent time evolution sequence before subduction zones can initiate at continent margins. We never see subduction initiation at continent margins until an existing subduction zone, that initiated elsewhere, migrates toward and impacts one of the margins. Only after the first one or two impact events during the model evolution of an existing subduction zone to the continent margin do we then see later subduction initiation directly at the margin. For the rest of the models' evolution subduction then initiates in roughly equal proportions at the continent margin or far from the margin. We propose that migration of an existing subduction zone to the continent margin advects a weak damaged zone, that then anchors at the margin. This zone of weakness persists and can then facilitate later subduction initiation at the margin. However, this time progression indicates that the stresses imposed by the continent itself were insufficient to drive enough grain size reduction for subduction initiation on their own.

So far, we have focused on whether continents change the convection regime from stagnant to mobile lid or control subduction initiation locations. But, exploring models that would have been in a mobile lid regime even without continents provides additional insight. If continents play a significant role in subduction initiation, then the presence of continents should enhance lithospheric damage, which can in turn increase plate speeds due to weaker plate boundaries. We, therefore, look at how lithospheric damage and plate speed are influenced by the presence of a continent and continental thickness. As explained above, we expect thicker continents to result in higher lithospheric stresses, and hence drive enhanced damage. We test this expectation by analyzing the average horizontal surface velocity (roughly representing a plate velocity) and average fineness in lithospheric shear zones in our models.

We calculate the time average surface horizontal velocity by first taking a spatial average of the horizontal velocity at the top nodes of the model domain, representing the surface, at each timestep and then time-averaging after the model has reached statistical steady state. We also calculate a time average of the maximum fineness throughout the whole model domain at each timestep, which represents the damage in actively deforming shear zones. If the stresses provided by continents are significant and scale with continent size, we expect to see significantly increased lithospheric fineness and surface velocity, with an increasing trend with continental thickness. However, we do not see significant increases in time-averaged surface horizontal velocity or fineness in our models when continents are added or a trend of increasing fineness or velocity with increasing continent thickness (See Figure 4). For all internal heating rates, the surface horizontal velocity remains constant regardless of continental thickness, approximately equal to the values seen in models without continents. Similarly, maximum fineness also does not increase with continents included. The trend with continent thickness is more random and even appears to show decreasing fineness with increasing continent thickness in some cases. We also apply the same averaging to the models with lower θ_h that are closer to the regime boundary and obtain the same result. The continent does not have a significant impact on both the surface horizontal velocity and maximum fineness. In all cases, the time-averaged maximum fineness with continents included is actually lower than in the case where continents are not included. We propose that the decrease in fineness when continents are added is due to the weakening and eventual vanishing of subduction zones as they migrate to the continental margins, seen commonly in our models. When time averaging over the model run time we capture this weakening, which is absent without continents, and consequently compute slightly diminished time-averaged fineness values with

Overall, the model results indicate a generally weak effect of continents on lithospheric damage and subduction initiation. We do not see continent margins serving as preferred locations for subduction initiation, nor enhanced damage in the lithosphere or surface plate speeds. The only impact of continents our models do show is that some models switch from stagnant-lid to mobile-lid convection for very thick continents and for parameters very close to the boundary between regimes found without continents. The model results then suggest that continents are not significantly boosting stress and deformational work in the lithosphere above what global scale mantle convection provides. To better contextualize and explain the convection model results, as well as more directly apply the results to potential subduction initiation on the early Earth, we next derive a scaling law for stress enhancement from a continent.

4. Scaling Analysis

To derive a scaling law for lithospheric stress enhancement due to the presence of a continent, we use simple models that isolate the continent's effect. To do this, we model a continent included in a laterally homogeneous

CHOI AND FOLEY 11 of 25

21699356, 2024, 10, Downloaded from https://agupubs.onlinelibrary.wiley.com/doi/10.1029/20241B029136, Wiley Online Library on [31/05/2025]. See the Terms and Conditions (https://onlinelibrary.wiley.com

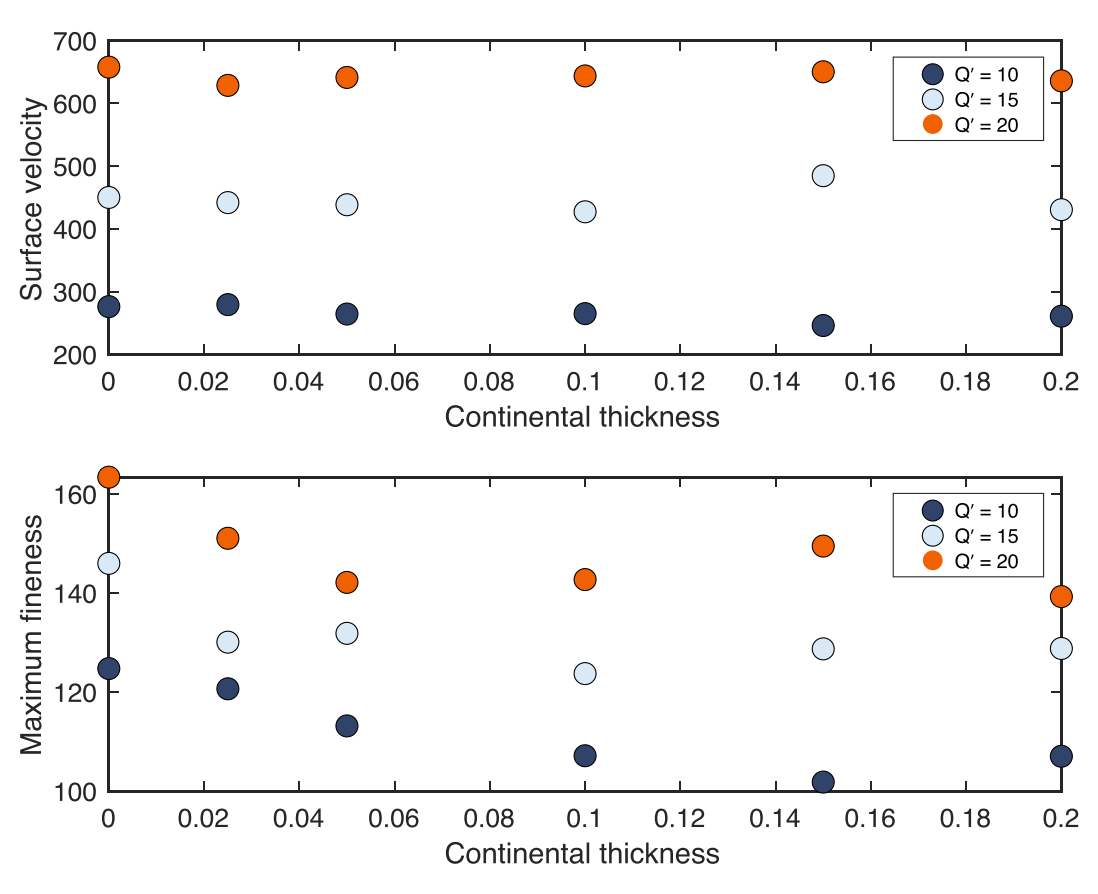


Figure 4. Time averaged surface horizontal velocity (top) and maximum fineness (bottom) as a function of continent thickness. Other parameters for this set of models are Q'=10,15, and 20 as indicated by the legend, $\theta_h=13.82$, and $\mu_{\text{jump}}=100$.

mantle with a temperature that follows an error function with depth, and zero initial velocity field (i.e., v'=0 at t'=0). The use of zero initial velocity field is to keep stresses from global-scale convection from masking the role of the continent. A plate age of ≈ 0.0024 (in non-dimensional units) is used in the error function, which sets the overall non-dimensional lithospheric thickness in the model to 0.099. Viscosity in these models is solely temperature-dependent and grain size evolution is not included. This allows the models to focus solely on the lithospheric stresses imposed by the continent, removing the complicating feedback of grain size evolution on lithospheric stress. The models vary the key parameters Rayleigh number, continent thickness, viscosity Frank-Kamenetskii parameter, and the compositional viscosity increase of the continent compared to the surrounding mantle. Specifically, Ra is varied from 10^5 to 10^8 , covering the range commonly used in previous studies for Archean conditions (Lenardic, 1997; Lenardic et al., 2003; O'Neill et al., 2013; Wang et al., 2018), and a wide enough range for developing a scaling law. Viscosity Frank-Kamenetskii parameter, θ_{ν} , was varied over a range of 6.908–16.12, which leads to viscosity ratios between surface and mantle of $10^3 - 10^7$. For the continent characteristics, we explored a range of d_{cont} from 0 up to 0.2, as we did in our full numerical models (again, this converts to 72.25-722.5 km, which more than covers possible continental lithosphere thicknesses in Archean and modern Earth). Finally, μ_{jump} was also varied from 1 to 100, which allows us to explore scenarios from very "mushy" continents (continents that have the same viscosity as mantle) to more rigid continent cases. We designated a baseline model with $Ra = 10^7$, $\theta_v = 13.82$, $\mu_{\text{jump}} = 100$, and $d_{\text{cont}} = 0.1$, and then varied each parameter one at a time over the given ranges, where other parameters are held fixed.

In these simple models, the only dynamic process is flow induced by the continent spreading under its own buoyancy, the rate of which is determined by the continent and surrounding lithosphere viscosity and Rayleigh number. If run long enough convection in the mantle would also develop, but as we focus solely on the flow and viscous stresses resulting from continental buoyancy, we stop models before convection develops. As the

CHOI AND FOLEY 12 of 25

21699356, 2024, 10, Downloaded from https://agupubs.onlinelibrary.wiley.com/doi/10.1029/2024JB029136, Wiley Online Library on [31/05/2025]. See the Terms and Conditions (https://agupubs.onlinelibrary.wiley.com/doi/10.1029/2024JB029136, Wiley Online Library on [31/05/2025]. See the Terms and Conditions (https://agupubs.onlinelibrary.wiley.com/doi/10.1029/2024JB029136, Wiley Online Library on [31/05/2025]. See the Terms and Conditions (https://agupubs.onlinelibrary.wiley.com/doi/10.1029/2024JB029136, Wiley Online Library on [31/05/2025]. See the Terms and Conditions (https://agupubs.onlinelibrary.wiley.com/doi/10.1029/2024JB029136, Wiley Online Library on [31/05/2025]. See the Terms and Conditions (https://agupubs.onlinelibrary.wiley.com/doi/10.1029/2024JB029136, Wiley Online Library.wiley.com/doi/10.1029/2024JB029136, Wiley Online Library.wiley.wiley.com/doi/10.1029/2024JB029136, Wiley Online Library.wiley.com/doi/10.1029/2024JB029136, Wiley Online Library.wiley.com/doi/10.1029/2024JB029136, Wiley Online Library.wiley.com/doi/10.1029/2024JB029136, Wiley Online Library.wiley.wiley.com/doi/10.1029/2024JB029136, Wiley Online Library.wiley.wi

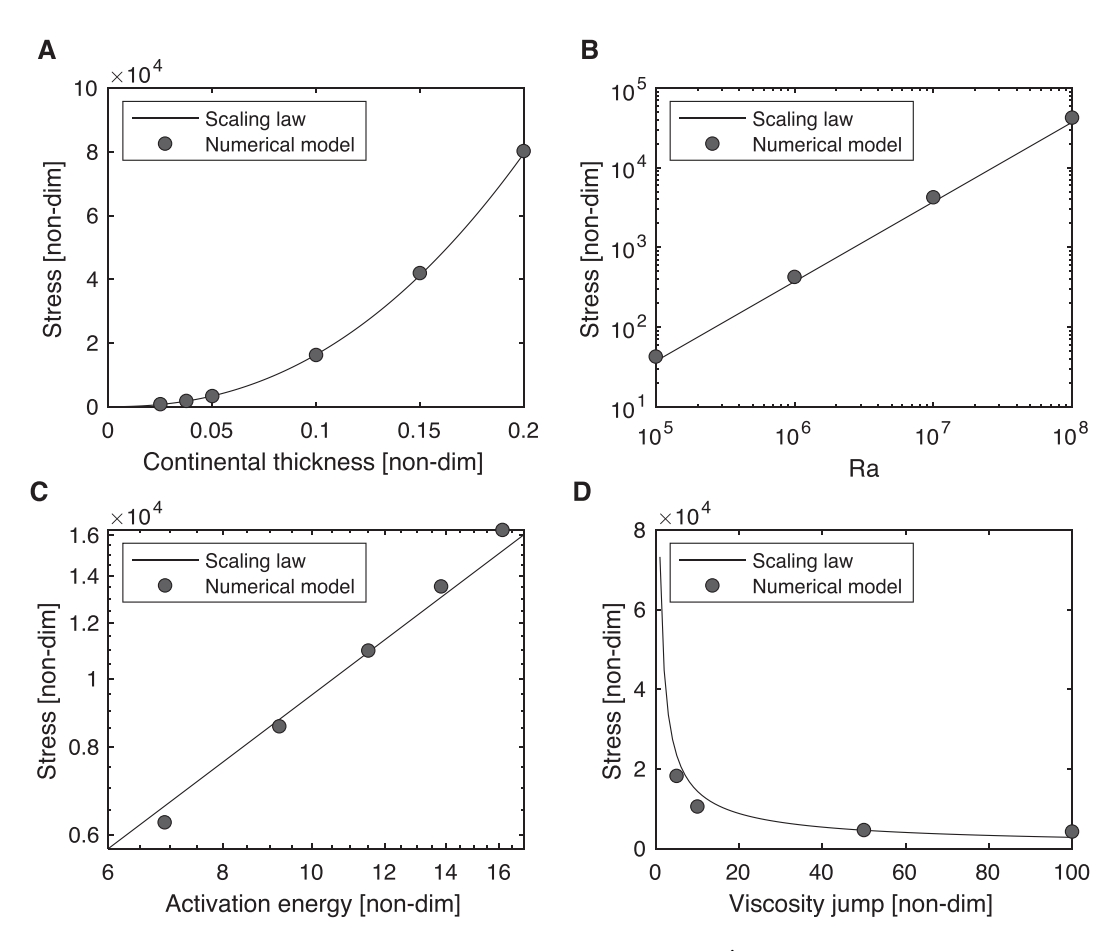


Figure 5. Lithospheric stress enhancement due to the presence of a continent, $\Delta \tau'$, as a function of model parameters (a) continent thickness (d_{cont}) ; (b) Rayleigh number (Ra); (c) viscosity Frank-Kamenetskii parameter (θ_{ν}) ; and (d) continent viscosity increase relative to the surrounding mantle (μ_{jump}) . The symbols are calculated from the models, and lines are power-law fits to the data points.

continent spreads and thins, viscous stresses decrease, so to quantify the maximum stress the continent can supply to the lithosphere, we analyze the first time step. We spatially average the second invariant of the stress tensor for all surface nodes except for within the continent, then define this as the "stress enhancement" due to the continent. The results of our simple models show that the viscous stress due to the continent increases with higher Ra, $d_{\rm cont}$, θ_{ν} , and decreases with higher $\mu_{\rm jump}$ (Figure 5).

Based on the simple model results, we develop a scaling law for the stress induced by a continental block as a function of the following model parameters: $d_{\rm cont}$, Ra, θ_{ν} , and $\mu_{\rm jump}$. The model results indicate approximate power law relationships between stress enhancement from the continent and the model parameter being varied. We therefore developed empirical power law fits between stress enhancement and each parameter as shown in Figure 5. Combining these individual power laws fits into a single scaling law for the stress enhancement due to a continent, $\Delta \tau'$, gives:

$$\Delta \tau' = 0.2764 \cdot Ra \cdot d_{\text{cont}}^{2.6643} \cdot \theta_{\nu}^{1.228} \cdot \mu_{\text{jump}}^{-0.57}. \tag{13}$$

Thicker continents have larger net buoyancy forces, resulting in a stronger driving force for continent spreading and hence higher compressive stress acting on the surrounding lithosphere, as our scaling law reflects with a strong positive dependence of $\Delta \tau'$ on d_{cont} . We also find that increasing θ_{ν} increases $\Delta \tau'$, because higher θ_{ν} leads to larger viscosity in the lithosphere, and viscous stress increases linearly with viscosity. On the other hand, higher viscosity contrast between continents and surrounding mantle leads to a more rigid continent less able to spread and push against the surrounding lithosphere; the result is a decrease in stress enhancement. Equation 13 also

CHOI AND FOLEY 13 of 25

21699356, 2024, 10, Downloaded from https://agupubs.onlinelibrary.wiley.com/doi/10.1029/2024JB029136, Wiley Online Library on [31/05/2025]. See the Terms and Conditions (https://online

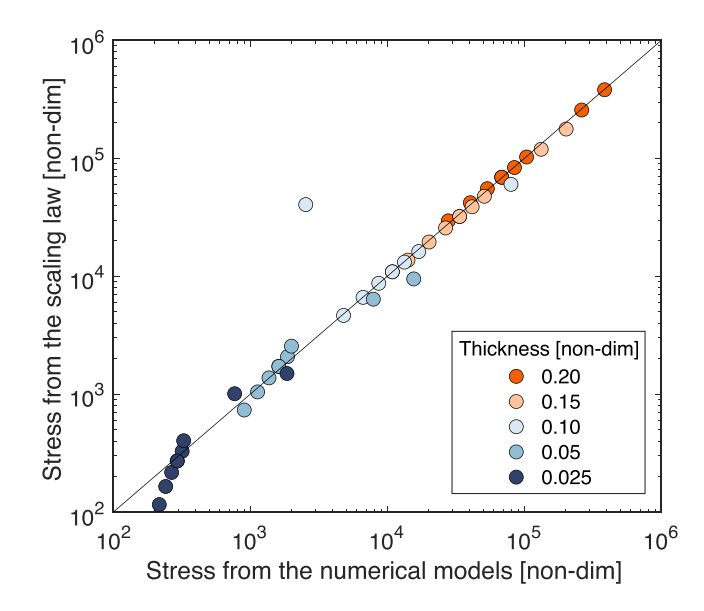


Figure 6. Comparison between lithospheric stress enhancement, $\Delta \tau'$, calculated from the scaling law and observed in the simple models of continent spreading. The black line plots x = y, the line upon which symbols should line up if the scaling law is accurate. For all but the lowest continent thickness, data points clearly cluster along the x = y line, indicating that our scaling law represents most models well.

demonstrates that the stress enhancement is proportional to Ra. Higher Ra increases the buoyancy force of density differences in the system. Therefore, it increases the buoyancy force of the continent, thereby increasing stress.

A joint comparison of the full scaling law to the whole suite of simple continent spreading model results shows the scaling law is accurate (Figure 6). Most results line up on the x = y line regardless of continental thickness or other parameters, which means there is a good agreement between scaling law and model results in general. However, there is a noticeable deviation from the x = y line at lower continent thicknesses, $d_{cont} = 0.025$ and 0.05. Specifically, the scaling law tends to underestimate stress enhancement in these thinner continent models. This is because the scaling relationship between $\Delta \tau'$ and θ is more complicated in reality: while we use a constant value for the exponent, when fitting the model results we found that the exponent itself is a weak function of continent thickness. While this relationship is interesting, fully working it out is beyond the scope of this paper, so we develop a scaling law that can best fit the majority of models across the range of continent thicknesses tested. Although further work would be needed to confirm, we hypothesize that the deviation in the scaling at low continent thicknesses is caused when continents are thinner than the surrounding oceanic plate. On Earth, we expect continents to be thicker than typical oceanic lithosphere, so our scaling law is developed to fit the thicker continent models where such a geometry is realized geometry.

To assess the relevance of the scaling law developed from the simple models that only consider continent extension as a source of deformation, we compare the predicted $\Delta \tau'$ from our scaling law to that observed in the full

numerical convection models with damage from Section 3. We determine lithospheric stress in the full convection models by recording stress values from the model's surface nodes, except where the continent is located, at time increments of $\approx 10^{-4}$ in non-dimensional units. At each time increment, the stress in the non-continent lithosphere is spatially averaged, and then this spatial average is time averaged over the model run, resulting in the black points in Figure 7. We also constrain the variability around this average stress by taking the minimum and maximum lithospheric stress at each time increment, and time averaging these as well. The average minimum and maximum stress is represented by black error bars. Note that in our full convection models, thick continents thin over time as their positive buoyancy leads to some lateral spreading. To better compare with the scaling law, we, therefore, redefined continent thickness to that reached at an approximate steady state. As there is no direct way to calculate $\Delta \tau'$ in the full convection models, we instead convert the scaling law for $\Delta \tau'$ into total lithospheric stress, τ' , by adding $\Delta \tau'$ from the scaling law to the average lithospheric stress seen in full convection models without continents, with the same set of input parameters.

We plot τ' from the scaling law as a function of continent thickness compared to the range of lithospheric stresses seen in the full convection models (Figure 7). The scaling law prediction for lithospheric stress increases sharply with continent thickness, as discussed above. However, the full numerical models show lithospheric stress is relatively insensitive to continent thickness, regardless of internal heating rate. As a result, τ' calculated from the scaling law is within the range of observed stress in the full convection models for thin continents up to $d_{\rm cont}=0.1$ for all internal heating rates. Specifically, the scaling law predictions tend to be higher than the average, toward the upper bound of stress from the convection models. However, with the strong influence of continent thickness in the scaling law, the predictions diverge from the convection model results at high continent thickness, with the scaling law overpredicting stress compared to the convection models. A potential explanation for this is that damage helps relieve stress in the models by weakening the adjacent oceanic lithosphere. Ultimately, the comparison of the scaling law to the full convection models shows that the scaling law will, if anything, overpredict the increase in stress from including continents. As a result, further analysis of our scaling law will provide an upper bound on the effect of continents on lithospheric damage and subduction initiation.

CHOI AND FOLEY 14 of 25

21699356, 2024, 10, Downloaded from https://agupubs.onlinelibrary.wiley.com/doi/10.1029/20241B029136, Wiley Online Library on [31/05/2025]. See the Terms and Conditions (https://online

library.wiley.com/terms-and-conditions) on Wiley Online Library for rules of use; OA articles are governed by the applicable Creative Commons License

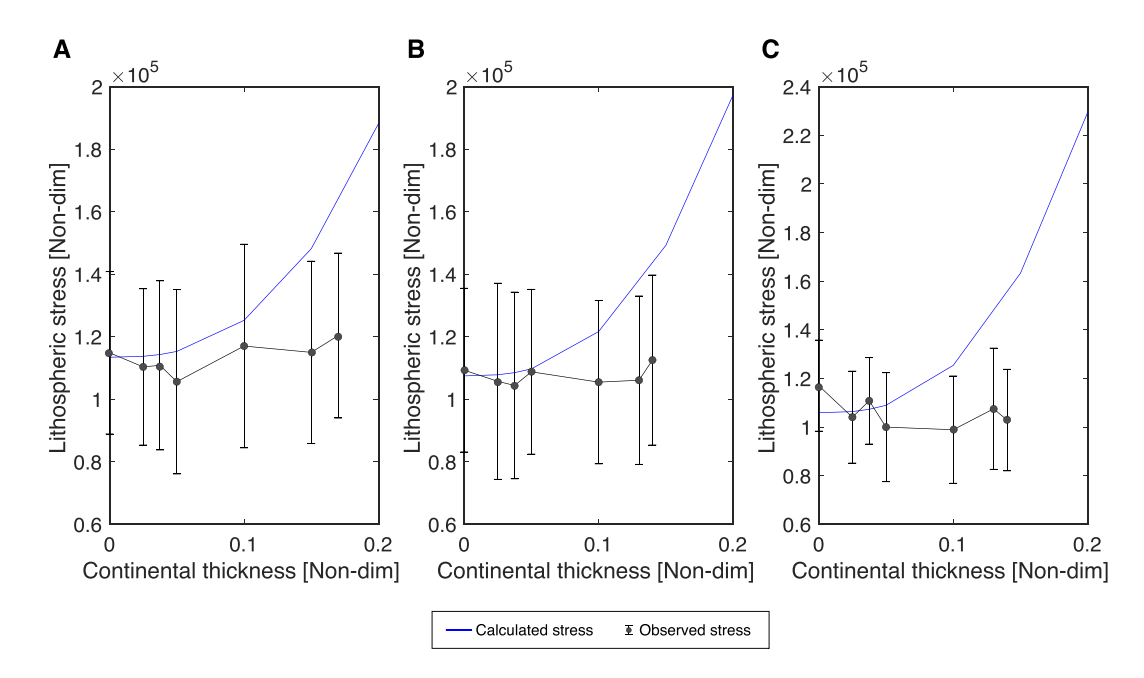


Figure 7. Comparison of predicted lithospheric stress, including stress enhancement due to the presence of a continental block, from the scaling law (Equation 13) to the results from the numerical convection models. (a) Lowest internal heating rate of Q' = 10, (b) Q' = 15, and (c) highest internal heating rate of Q' = 20. The dot represents the time average of spatially averaged lithospheric stress, and error bars are time averages of the minimum and maximum lithospheric stress (See main text for the details). The blue line shows the scaling law prediction for lithospheric stress, including the stress enhancement due to a continent of increasing thickness.

To further test whether the lithospheric stress enhancement from a continent is sufficient to significantly affect lithospheric damage and potentially trigger subduction initiation, we calculate the fineness that can be generated by lithospheric stress enhancement based on our scaling law. We specifically look at whether the stress enhancement from continents, $\Delta \tau'$, can produce enough lithospheric damage for subduction, meaning that we are testing whether continents on their own can produce enough stress for subduction initiation. We use our scaling law for $\Delta \tau'$, which may overpredict the stress enhancement in fully developed convection. As a result, continents driving subduction initiation will be even less likely in reality than our simple analysis here shows. To estimate the lithospheric damage that can be caused by continental stress enhancement, we take the fineness evolution equation, Equation 2, in steady-state and assume that deformational work is entirely caused by continent stress enhancement, $\Delta \tau'$. The rate of deformational work, $\Psi = \underline{\underline{\dot{\varepsilon}}} : \underline{\tau}$. Using the viscous constitutive law, $\underline{\tau} = 2 \mu \underline{\dot{\varepsilon}}$ and the definition of the second invariant of the stress tensor, $\tau = \sqrt{(1/2)\tau_{ij}\tau_{ij}}$, then for a general stress tensor $\underline{\tau}$

$$\Psi = \frac{\tau^2}{\mu}.\tag{14}$$

If we replace the work rate from Equation 2 using Equation 14 and assume steady-state, then:

$$\frac{f}{\mu\gamma}\tau^2 = hA^p \tag{15}$$

As we are calculating lithospheric damage, we use the viscosity and healing rates for lithospheric temperature, $\mu = \mu_l (A/A_0)^{-m}$ and $h = h_l$, where μ_l and h_l are the temperature-dependent components of the viscosity and healing rate, respectively, evaluated at a lithospheric temperature, T_l . With these definitions:

$$\frac{f\tau^2}{\mu_l \gamma} \left(\frac{A}{A_0}\right)^m = h_l A^p \tag{16}$$

which can be solved for A to give:

CHOI AND FOLEY 15 of 25

Non-dimensionalizing Equation 17 using the same scaling factors as in Section 2.2 and replacing the general stress invariant with the continental stress enhancement, $\Delta \tau$, gives the fineness that can be caused by continental buoyancy forces:

$$A'_{\rm sz} = \left(\frac{D\Delta\tau^2}{Hh'_l\mu'_l}\right)^{\frac{1}{p-m}} \tag{18}$$

where $h'_l = \exp(-\theta_h)$ and $\mu'_l = \exp(\theta_v)$ assuming that the surface temperature of T' = 0 in our numerical convection models represents the temperature of the lithosphere, T'_l . We apply the analysis here directly to our numerical convection models, so we use the same linear-exponential temperature-dependent form of viscosity and healing as in the numerical models. Because the models we apply the scaling analysis to have different internal heating rates that lead to different mantle temperatures and different average fineness in the mantle interior, we use an internal Rayleigh number, Ra_i , in calculating $\Delta \tau'$:

$$Ra_i = Ra_0 \frac{T'_{\text{man}}}{\mu'_{\text{man}}} \tag{19}$$

where $T'_{\rm man}$ is the time-averaged mantle interior temperature calculated from each model in a post-processing step, and $\mu'_{\rm man}$ is the average mantle interior viscosity: $\mu'_{\rm man} = \exp(\theta_v (1-T'_{\rm man})) A'_{\rm man}^{-m}$, where $A'_{\rm man}$ is the time-average mantle interior fineness from each model. Moresi and Solomatov (1998) suggest that the viscosity of oceanic lithosphere needs to be reduced to no more than 3×10^3 times the underlying mantle to initiate subduction. In other words, if the viscosity of a lithospheric shear zone $(\mu_{\rm sz})$ is less than 3×10^3 the underlying mantle viscosity $(\mu_{\rm man})$, subduction can initiate. To determine if continents on their own can lead to subduction initiation, we estimate whether this requisite viscosity reduction can be achieved based on Equation 18. We calculate the non-dimensional shear zone viscosity as $\mu'_{\rm sz} = \mu'_l A'_{\rm sz}^{-m}$ and the non-dimensional mantle viscosity, $\mu'_{\rm man}$, as given above. We apply the estimate of $\mu_{\rm sz}/\mu_{\rm man}$ to our convection model results from Section 3, using $D=10^{-2}$, $H=1.5\times10^5$, $\theta_{\rm v}=13.82$, and $\theta_{\rm h}=13.82$ as in the full convection models.

The calculated lithospheric fineness and $\mu_{\rm sz}/\mu_{\rm man}$ that can be expected due to continental stress enhancement in our full convection models, based on the scaling analysis developed here, are shown in Figure 8. Clearly, the damage induced by continental stress enhancement is not enough on its own to initiate subduction, as shear zones can not be weakened sufficiently (Figure 8b). Even with a very thick continent of $d_{\text{cont}} = 0.2$ and high internal heating of Q' = 20, only a fineness range of $A'_{\text{cont}} \approx 19 - 32$ can be generated, resulting in $\mu_{\text{sz}}/\mu_{\text{man}} \sim 10^4 - 10^5$; too large for subduction initiation. Meanwhile, subduction zones in the convection models generated by deformational work induced by global scale mantle flow feature much larger fineness, usually well above 100. The largest values of fineness driven by continental stress enhancement we estimate result from models with higher internal heating rates where convection is more vigorous, increasing $\Delta \tau'$. However, higher internal heating rates also act to lower μ'_{man} through higher mantle temperatures, so μ_{sz}/μ_{man} then does not scale straightforwardly with $A'_{\rm sz}$. Note that very large $\mu_{\rm sz}/\mu_{\rm man}$ are observed in low $d_{\rm cont}$ models. This can be attributed to the low stress resulting in large grains and high μ'_{sz} . In reality deformation would likely switch to being dominated by dislocation creep at such large grain sizes, keeping μ'_{sz} from rising so sharply. However, the general trend that larger continents can drive more damage and hence lower μ_{sz}/μ_{man} still holds, as well as the finding that even thick continents do not cause enough damage to initiation subduction in our models. The scaling analysis presented here therefore illustrates why including continents had minimal effect on subduction initiation and lithospheric damage in our full convection models; the stress enhancement provided by a continental block is not sufficient to drive significant damage.

CHOI AND FOLEY 16 of 25

21699356, 2024, 10, Downloaded from https://agupubs.onlinelibrary.wiley.com/doi/10.1029/2024JB029136, Wiley Online Library on [31/05/2025]. See the Terms

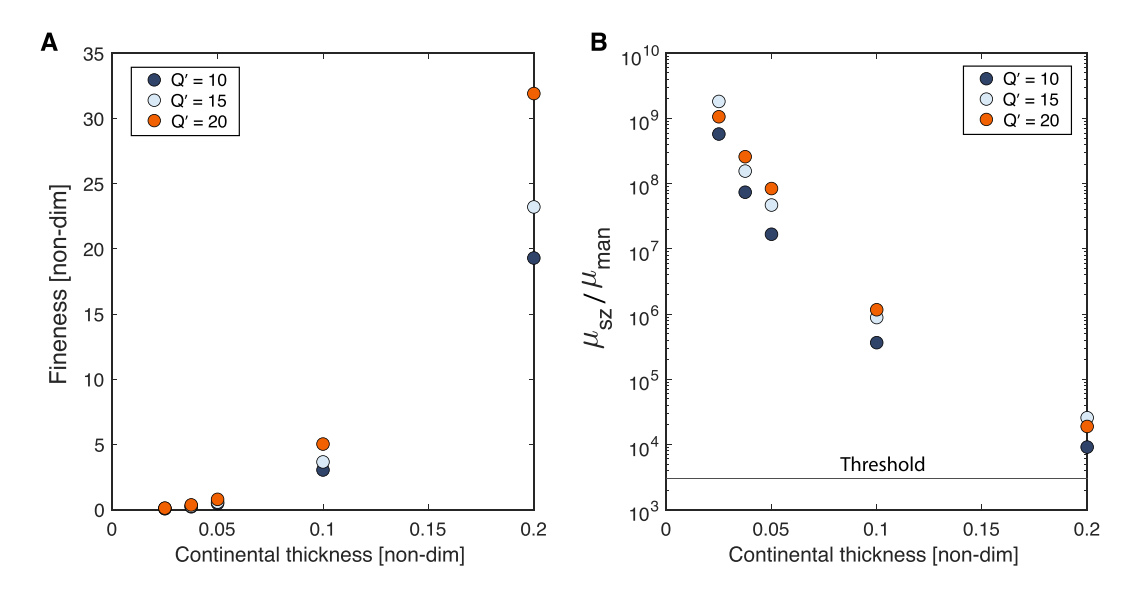


Figure 8. (a) Calculated fineness due to the continental stress enhancement. (b) Calculated ratio between the viscosity of a plate boundary, or shear zone, and the viscosity of the underlying mantle (μ_{sx}/μ_{man}) due to damage driven by continent stresses. The black line indicates a threshold below which subduction initiation is possible based on previous studies.

5. Application to Subduction Initiation in the Archean

Although our numerical models find that continents have only a limited ability to drive subduction initiation, they are, of course, not perfect representations of realistic Earth conditions. Viscosity variations in particular could be many orders of magnitude larger on the real Earth than what can be reasonably achieved in numerical models. Therefore, that continental blocks do not provide sufficient stress on their own to initiate subduction in our numerical models does not mean it could not happen on the real Earth. To test this possibility, we apply our scaling law developed in Section 4 to early Earth conditions. Scaling relationships like our Equation 13 can be extrapolated to more realistic Earth conditions, allowing for a simple estimate of the system behavior in these cases. As in Section 4, we will consider the continental stress enhancement to be the only source of stress, to determine if continents on their own can drive subduction initiation on the Archean Earth, or whether stresses provided by global-scale mantle convection are more important.

As in Section 4, we estimate the lithospheric fineness that results from the continental stress enhancement, with the fineness evolution equation in steady-state. In dimensional variables, this gives

$$A_{\rm sz} = \left(\frac{f\Delta\tau^2}{h_l \mu_l \gamma A_0^m}\right)^{\frac{1}{p-m}} \tag{20}$$

where $\Delta \tau$ is continental stress enhancement in dimensional units. As we apply the scaling analysis to the Archean Earth, we use more realistic Arrhenius relationships for the viscosity and healing terms

$$\mu_l = \mu_0 \exp\left(\frac{E_v}{RT_l}\right),\tag{21}$$

$$\mu_{\text{man}} = \mu_0 \exp\left(\frac{E_v}{RT_{\text{man}}}\right),\tag{22}$$

$$h_l = h_0 \exp\left(-\frac{E_h}{RT_l}\right),\tag{23}$$

CHOI AND FOLEY 17 of 25

21699356, 2024, 10, Downloaded from https://agupubs

ibrary.wiley.com/doi/10.1029/2024JB029136, Wiley Online Library on [31/05/2025]. See the Terms

Figure 9. Calculated ratio between the viscosity of a plate boundary, or shear zone, and the viscosity of the underlying mantle $(\mu_{\rm sz}/\mu_{\rm man})$ due to damage driven by the enhanced lithospheric stresses provided by a continent at Archean conditions $(T_{\rm man}=1800{\rm K})$. The black line indicates a threshold where subduction initiation is possible based on our calculation. The dashed line shows how the threshold for subduction initiation would shift if the continent stress enhancement is higher than our scaling law, as implied by Rolf and Tackley (2011).

This study - - Stress implied by Rolf and Tackley (2011)

where $T_{\rm man}$ and T_l are the temperatures of the mantle interior and the lithosphere, respectively. $T_{\rm man}$ is used to define the mantle interior viscosity, $\mu_{\rm man}$, as well as the Rayleigh number in the scaling law for $\Delta \tau$, and T_l is used to define the lithospheric viscosity and healing rate.

As in Section 4, we assume subduction can be initiated when the viscosity of lithospheric shear zones, μ_{sz} , satisfies $\mu_{sz}/\mu_{man} < 3 \times 10^3$. Lithospheric shear zone viscosity is defined as $\mu_{sz} = \mu_l (A_{sz}/A_0)^{-m}$. The final remaining terms to define are those in the continental stress enhancement scaling law (Equation 13): the Rayleigh number, Ra, and Frank-Kamenentskii parameter for viscosity, θ_{ν} . For application to the early Earth, we use the internal Rayleigh number.

$$Ra_i = \frac{\rho_o \alpha g(T_{\text{man}} - T_s) d^3}{\kappa \mu_{\text{man}}}$$
 (24)

and

$$\theta_{\nu} = \frac{E_{\nu}(T_{\text{man}} - T_s)}{RT_{\text{man}}^2}.$$
 (25)

The other terms in Equation 13, continent thickness and viscosity jump, will be taken as free parameters and varied over a range of $\mu_{\rm jump}=0.1$ to 100 and $d_{\rm cont}=0.01$ to 0.5.

As we apply our analysis to the Archean, to assess whether the formation of initial continental blocks could trigger the initiation of subduction, we use $T_{\rm man}$ as estimated for the Archean Earth. Mantle temperature in Archean is estimated to range from 1725 to 1875 K based on petrological constraints

derived from Archean basalts (Herzberg et al., 2010). We therefore adopt $T_{\rm man}=1800{\rm K}$ in our analysis. Also important is the lithospheric temperature, T_l , meant to represent the temperature of the mid-lithosphere where strength is highest. We use $T_l=900{\rm K}$, consistent with previous studies (Bercovici & Ricard, 2013; Foley, 2020). For the viscosity and healing terms, we use $E_v=300{\rm ~kJ/mol}$ and $E_h=430{\rm ~kJ/mol}$ (see Sections 2.1 and 2.3). For the pre-exponential constants, μ_0 is calculated by plugging present-day values of $\mu_{\rm man}=4\times10^{21}{\rm ~Pa\cdot s}$ and $T_{\rm man}=1630{\rm ~K}$ into Equation 21, resulting in $\mu_0=9.7269\times10^{11}{\rm ~Pa\cdot s}$ and h_0 is determined by using Equations 11 and 12 from Foley (2018a) as $\mu_0=9.7269\times10^{11}{\rm ~and}$ $h_0=1.0851\times10^{-9}.h_0=1.0851\times10^{-9}$ as in Foley (2018a).

We calculate the ratio $\mu_{\rm sz}/\mu_{\rm man}$ as a function of continent thickness and viscosity jump (Figure 9), with a solid line denoting the critical value below which subduction initiation is possible. Our calculation suggests both thicker continents (higher $d_{\rm cont}$) and lower continent viscosity (lower $\mu_{\rm jump}$) lead to higher stress and more damage, and therefore a smaller ratio of $\mu_{\rm sz}/\mu_{\rm man}$. The results show that subduction initiation solely due to the presence of continents would require unrealistically thick or low-viscosity continents. For $\mu_{\rm jump}=1$, that is continents have the same intrinsic viscosity as the surrounding mantle, the continent would need to be at least 250 km thick. However, both seismic tomography (Steinberger & Becker, 2018) and diamond-bearing kimberlites (Finnerty, 1987) studies suggest that the continental lithospheric mantle cannot be thicker than 200–250 km. Moreover, with $\mu_{\rm jump}=1$, mantle dynamics studies indicate continental blocks can not survive entrainment by global-scale convection, as cratons on Earth have (Lenardic & Moresi, 1999; Lenardic et al., 2003). Instead, $\mu_{\rm jump}=100-1000$ is needed for craton survival; at these values continents would need to be 700 km thick to initiate subduction, well above observational constraints. Only if continents have a lower intrinsic viscosity than the surrounding mantle ($\mu_{\rm jump}<1$) can continents with a realistic thickness trigger subduction, but there is no known mechanism that produces continents, in particular continental lithospheric mantle, that is rheologically weaker than surrounding mantle.

CHOI AND FOLEY 18 of 25

21699356, 2024, 10, Downloaded from https

ibrary.wiley.com/doi/10.1029/2024JB029136, Wiley Online Library on [31/05/2025]. See the Terms

As discussed further in Section 6.1, based on a comparison to previous studies using a plastic yield stress rheology, it is possible our scaling law underestimates continental stress enhancement by up to a factor of 3.6. An additional factor that could impact the results is the deviation from our scaling law found for models with $d_{\rm cont}=0.025$, shown as dark-blue dots in Figure 6. If we recalculate the final scaling law to fit the $d_{\rm cont}=0.025$ models, we find $\Delta \tau$ also increases overall, but less than the factor of 3.6 we infer from comparing to studies with a pseudoplastic rheology. We therefore assume that the maximum amount by which our scaling law could be underpredicting continental stress enhancement is a factor of 3.6, and so recalculate the threshold for subduction initiation by multiplying our equation for $\Delta \tau$ by 3.6 (dotted line in Figure 9).

However, even with this larger continental stress, the continent thickness and viscosity jump range required for subduction initiation are still not realistic: continents with a realistic $\mu_{\text{jump}} = 100$ would need to be thicker than 335 km, clearly exceeding observational constraints. Likewise, the only way continents with a realistic thickness of ~250 km can initiate subduction is if continents have a viscosity ≤ 8 times higher than the surrounding mantle, which makes survival of cratons for at least 2–2.5 Gyr timescales difficult. Therefore, we find the enhanced lithospheric stresses provided by continents cannot initiate subduction on the Archean Earth. Instead, other factors such as cooling mantle and surface temperatures may have been more important for allowing weak shear zones to develop and plate tectonics to initiate (Foley et al., 2014).

6. Discussion

We have implemented a continental block into models of mantle convection with grain-damage and found at most minor stress enhancement at the continental margins. We find that the lithospheric stress enhancement provided by continents is largely due to their spreading outwards under their positive buoyancy. This stress enhancement can drive minor amounts of lithospheric damage, and for very thick continents this is sufficient to induce a transition from stagnant-lid to mobile-lid convection for a small region of parameter space very close to the regime boundary as found without continents. However, in most cases, our models show continents have no strong effect on lithospheric damage, neither boosting grain size reduction or surface mobility nor dictating sites of subduction initiation. Our scaling analysis further shows that continental buoyancy forces are not sufficient to initiate subduction at early Earth conditions unless continents have unrealistically low intrinsic viscosity or large thickness.

Our models, however, make some simplifications in order to facilitate the analysis of their results and keep calculations numerically tractable. These simplifications could impact some of the primary results. We assumed a rectangular initial shape for continents in our model, while shapes are almost certainly more complex on the real Earth. However, the actual shape of Earth's early continents is not constrained, and it is unclear if the geologic record contains the information needed for such a constraint. We view the simple rectangular shape used in our study as sufficient to examine first-order behavior. However, as discussed further in Section 6.1 below, it is possible that angled sides to the continents, rather than vertical as in our rectangular continents, would facilitate the outward spreading of the continent and the initiation of subduction. Another simplification is our use of a twodimensional Cartesian model, while the Earth is inherently three-dimensional spherical. Studies of plate generation without continents have generally found that two-dimensional versus three-dimensional and cartesian versus spherical geometry does not significantly change where stagnant-lid and mobile-lid behavior is seen, at least with a plastic yield stress rheology (e.g., Tackley, 2000b; Van Heck & Tackley, 2008; Weller & Lenardic, 2012). Our models also assume a constant buoyancy number across all models and through model evolution. The chosen value is consistent with estimates based on the depth average compositional density through modern continents. However, the composition of continents could evolve over time, from more mafic in the early Archean to more felsic by the end of the Archean (Tang et al., 2016). Such compositional change would lead to lower Bu on the early Earth than used in our models, as continents would be less buoyant with a more mafic composition. Lower Bu would make continents even less impactful on lithospheric stresses and subduction initiation.

Furthermore, this study focuses on exploring lithospheric stress enhancement by a continent using grain-damage rheology. Consequently, our models are purely viscous and only consider grain size reduction as a mechanism for creating weak plate boundaries. Other rheologies, like plasticity, are not included, as discussed previously; we compare our results to models using a plastic yield stress rheology below in Section 6.1. We also do not consider the effects of elasticity, which could potentially influence stress distribution and subduction initiation. Elasticity has been suggested to facilitate significant stress accumulation that promotes brittle failure of the lithosphere

CHOI AND FOLEY 19 of 25

21699356, 2024, 10, Downloaded from https://agupubs.onlinelibrary.wiley.com/doi/10.1029/2024JB029136, Wiley Online Library on [31/05/2025]. See the Terms

(Beuchert & Podladchikov, 2010). However, Zhou and Wada (2022) argued the effectiveness of elasticity in subduction initiation is conditional, being more significant with large thermal age contrasts between overriding plate and subducting plate and lower convergence rates. Patočka et al. (2019) also suggested that including elasticity would not strongly impact results on subduction initiation. Moreover, the influence of elasticity is believed to be more significant after subduction has developed, rather than its initiation (Zhou & Wada, 2022), which is beyond the scope of our study.

6.1. Comparison to Previous Studies

Our findings of the minimal influence of continents on subduction initiation are in contrast to some previous studies (Rey et al., 2014; Rolf & Tackley, 2011), which find more significant stress enhancement due to the effects of continents, such that continents could meaningfully trigger subduction initiation and surface mobility. Therefore, here we discuss the key differences in the models that might lead to these different conclusions.

Rey et al. (2014) modeled lateral spreading of an implemented buoyant continent. They used the results to argue that Archean conditions would lead to significant spreading, compressing and forcing downward the surrounding ocean lithosphere until subduction is triggered. The ability of this continental spreading to weaken the surrounding lithosphere and trigger subduction initiation is the biggest difference between our results and theirs. The amount of continent spreading in our models with thick continents is similar to that seen in the models of Rey et al. (2014), before subduction initiation. In Figure 1b of Rey et al. (2014), the time just before subduction initiation, the continent has spread to $\sim 160\%$ of its initial width and thinned to $\sim 60\%$ of its initial thickness. Meanwhile in our models we see continents spreading up to $\sim 190\%$ of the initial width and thinning to $\sim 68\%$ of the initial thickness. Further continent spreading up to $\sim 250\%$ of the initial width and thinning to $\sim 50\%$ of the initial thickness only occurs after subduction has initiated in Rey et al. (2014) (see their Figure 1), likely driven by the pulling force exerted by the downwelling slab on the continent.

Given that we see a similar amount of continent spreading in our models as Rey et al. (2014) sees before subduction initiates in theirs, we hypothesize that the different rheological models employed is the primary factor explaining the different results. Rey et al. (2014) utilized a plastic rheology incorporating a weakening factor dependent on plastic strain to generate localized plate boundaries. This approach results in a decrease in the friction coefficient with increasing strain. As their modeled continent spreads and deforms, the friction coefficient reduces near the continental margins, allowing subduction to initiate in their model. Our model of forming plate boundaries through grain size reduction also effectively includes a type of strain weakening, as grain size reduction is driven by deformational work, a product of strain rate. However, as demonstrated with our models and scaling analysis, the stress and deformation induced at continent margins are not enough on their own to initiate subduction through grain size reduction.

In addition, different continent geometries could also play a secondary role in the different results. We use a simple rectangle as a continent, while Rey et al. (2014) used an upside-down right trapezoid as a continent with angles that can naturally force the oceanic lithosphere down as it spreads. As the positive buoyancy of the continent favors spreading outward along the upper boundary of the model domain, the trapezoidal shape facilitates spreading and, by forcing the surrounding ocean lithosphere downward, subduction initiation.

Another important comparison point is to Rolf and Tackley (2011), who found that including continents significantly expanded the mobile lid regime with a plastic yield stress rheology. With the yielding model, the shift in stagnant-lid to mobile-lid regime boundary to higher stresses with continents included can be used to provide a rough estimate of continental stress enhancement. The reason being that to produce mobile-lid convection with a plastic yield stress model, convective stresses must reach the yield stress, and therefore the upper bound on yield stress that allows mobile-lid convection implies an upper bound on convective stress. The regime diagram from Rolf and Tackley (2011) therefore indicates that adding continents increases stress by ~240 MPa. We can then use our scaling law for stress enhancement to calculate the stress enhancement we would predict for their models as a simple comparison. Using the model parameters from Rolf and Tackley (2011) ($d_{\text{cont}} = 0.2$, $\theta_{\nu} = 11.513$, $\mu_{\text{jump}} = 100$, $Ra = 10^6$, Q' = 20.5), we calculate $\Delta \tau = 5.526 \times 10^3$ from our scaling law (Equation 13). Q' here does not affect our scaling law, but we note it as one of the key parameters in Rolf and Tackley (2011) that produces an internal mantle temperature of ~1 in non-dimensional units. Converting this stress back to dimensional units ($\tau = \tau' \mu_m \frac{\kappa}{d^2}$, with $\mu_m = 10^{23}$ Pa·s as given in Rolf & Tackley, 2011), we obtain a

CHOI AND FOLEY 20 of 25

stress enhancement of \sim 66 MPa, which is smaller than that suggested by their regime diagram (\sim 240 MPa) by a factor of \approx 3.6.

One possibility with the discrepancy between stress enhancement predicted by our scaling law and that implied by Rolf and Tackley (2011) is that our models and scaling law are underpredicting stress enhancement. However, even if this is the case subduction initiation solely due to the continent is highly unlikely with Archean geologic parameters as we showed in Section 5. Even if we assume that continental stress enhancement is, in reality, a factor of 3.6 larger than our scaling law predicts, unrealistically low intrinsic viscosity or thick continents would be needed to trigger subduction initiation. Thus, we argue that subduction initiation in the Archean cannot be achieved primarily by continents. Instead, the tectonic regime would be controlled by other factors that affect grain-damage, such as surface temperature and convective vigor in the mantle (e.g., Foley, 2018b; Foley et al., 2014).

Ultimately, the comparison to previous studies demonstrates that the plastic yield stress and grain-damage models for generating plate boundaries are fundamentally different, and this can lead to different results for subduction initiation and tectonic regime (e.g., Foley, 2018b, see also Section 1). In the simple pseudo-plastic rheology used in Rolf and Tackley (2011), lithospheres fail once stress reaches the yield strength, leading to a one-to-one relationship between lithospheric stresses and tectonic regime. However, with grain-damage the relationship is more complex. Stress leads to grain size reduction and subsequent weakening, then leading to development of subduction and a mobile-lid regime when a threshold viscosity reduction is reached. As a result, even with a consistent stress enhancement due to continents between our models and those of Rolf and Tackley (2011), whether such stress enhancement leads to subduction initiation could still differ. In Rey et al. (2014) the effective yield stress decreases as plastic strain accumulates, which also means that there is no longer a one-to-one relationship between convective stress and tectonic regime. Both convective stresses and accumulated plastic strain are important for determining whether plate tectonics can develop, which is similar to grain-damage, where the product of stress and strain rate drives grain size reduction. However, these mechanisms are still capturing fundamentally different physical processes and, therefore, still lead to different end results about the role of continents in subduction initiation.

The collective comparison with previous studies indicates that the choice of rheological model significantly influences whether continents play an important role in subduction initiation, and the global tectonic regime more broadly. Sensitivity to rheological models is not surprising, but is important to map out for making inferences about early Earth tectonics, as the rheological mechanisms that give rise to plate tectonics on Earth are not fully understood. Comparing different rheological models then highlights which geodynamical processes on early Earth are most sensitive to variations in rheological assumptions. While our results cannot rule out that continents could have been important for triggering subduction initiation on the early Earth, they do indicate that such a process is sensitive to the assumed lithosphere rheology.

Grain-damage and the plasticity models we compare to are also not mutually exclusive. Plasticity models are generally motivated to capture brittle faulting, while grain-damage is meant to capture viscous weakening of the mid-lithosphere. Future research efforts may benefit from integrating insights from both rheological frameworks to develop a more comprehensive understanding of subduction initiation and evolution in the early Earth.

6.2. Implications for the Geologic Record of the Acasta Gneiss Complex

Reimink et al. (2016) argued the transition from shallow melting to deeper melting in the AGC represents the formation of a continental nucleus through non-plate-tectonic processes, subsequently leading to the initiation of subduction at the margin of this continental block. Our models indicate that it would be difficult for continental blocks to trigger subduction initiation at their margins in the Archean when a grain-damage rheology is used. Our models therefore do not fully support the interpretation that the AGC records subduction initiation triggered by a continental nucleus. As discussed in Section 6.1, whether Archean continents can directly trigger subduction at their margins appears to be sensitive to the assumed rheology for forming weak plate boundaries. As such it is then important to consider alternative explanations to the geologic evidence that don't require a causative role for the continent nucleus in subduction initiation. We propose that the transition from shallow to deeper melting might just reflect the migration of a subduction zone that initiated elsewhere to the continent margin, after the formation of the continent nucleus. Examining geological evidence of subduction initiation at a margin, in contrast to the accretion or collision processes with an established subduction zone, would test this model.

CHOI AND FOLEY 21 of 25

21699356, 2024, 10, Downloaded from https://agupubs.onlinelibrary.wiley.com/doi/10.1029/2024JB029136, Wiley Online Library on [31/05/2025]. See the Terms and Conditions (https://onlinelibrary.wiley.com/terms-and-conditions) on Wiley Online Library for rules of use; OA articles are governed by the applicable Creative Commons Licens

7. Conclusions

We have explored the role of continents in the initiation of plate tectonics on Earth using numerical convection models with grain-damage. Contrary to previous suggestions that continents play a pivotal role in promoting subduction initiation through the enhancement of stresses and deformation near their margins, our study finds a significantly more muted role of continents. Our models demonstrate that adding a continental block into models of convection with grain-damage leads to some modest enhancement of stresses, such that very thick continents can trigger a shift from stagnant-lid to mobile-lid convection for a narrow region of parameter space near the regime boundary found without continents. However, for models that result in mobile lid convection without continents we see no enhancement of lithospheric damage and surface plate speeds with continents added, nor do we see subduction preferentially initiating at the continent margins. These findings indicate the boost in lithospheric stresses provided by the continent is not significant compared to stresses from underlying mantle convection in terms of driving grain size reduction.

We develop a simple scaling analysis for the enhancement in lithospheric stresses resulting from a continent. This scaling analysis is based off of simple models where a continent is placed in a mantle with zero initial velocity field, and stresses resulting from the positive buoyancy are analyzed throughout the lithosphere. The scaling analysis further demonstrates the limited role of a continent in driving subduction initiation with grain-damage, consistent with the results of our full numerical convection models. We apply our scaling analysis to Archean geologic conditions, and find that the stress provided by continents is not capable of triggering subduction initiation on its own. Therefore subduction initiation driven by the formation of continents on the early Earth would only occur if the planet was already very close to entering a mobile-lid regime anyway. Our findings show the importance of the rheology used for generating weak plate boundaries in making inferences about early Earth tectonic processes. With a plastic yielding rheology, previous studies find the enhancement of stress and deformation at continent margins is sufficient for triggering subduction initiation, while with grain-damage, we find it is not. Given the uncertainty in lithospheric rheology, our results then motivate alternative ideas for early Earth tectonics. Our results with grain-damage suggest that other factors may have been more important for subduction initiation in the early Earth, and the eventual development of plate tectonics. Geologic evidence indicating the formation of early continental blocks via non-subduction processes followed by deeper melting, potentially via subduction, may instead be the result of subduction zones migrating into the margins of continental blocks, rather than due to the block itself triggering subduction initiation at its margin. Future studies can explore this aspect by tracking the changing positions of subduction zones relative to continents over time.

Data Availability Statement

The mantle convection code (Foley, 2020) used for the study is available for download at GitHub (https://github.com/bradfordjfoley/foley-convection-code) and post-processing programs including the code used to produce figures are available for download at GitHub (https://github.com/heec12/post-conveco.git). Numerical model output is available upon request. The open-source software ParaView (v5.9.1) (Ahrens et al., 2005) used for numerical model visualization is available via https://www.paraview.org/download/ and corresponding code to convert our numerical model results into vtk file (ParaView readable format) is available for download at GitHub (https://github.com/heec12/conveco2vtk.git).

Acknowledgments

The authors thank the editor A. Friedrich and two anonymous reviewers for their constructive comments. This work was supported by NSF award EAR-1723057 and EAR-2046598.

References

Ahrens, J., Geveci, B., & Law, C. (2005). ParaView: An end-user tool for large data visualization. *Visualization Handbook*. Elsevier, ISBN-13: 9780123875822.

Bada, J. L., & Korenaga, J. (2018). Exposed areas above sea level on earth> 3.5 gyr ago: Implications for prebiotic and primitive biotic chemistry. Life, 8(4), 55. https://doi.org/10.3390/life8040055

Baes, M., Govers, R., & Wortel, R. (2011). Subduction initiation along the inherited weakness zone at the edge of a slab: Insights from numerical models. Geophysical Journal International, 184(3), 991–1008. https://doi.org/10.1111/j.1365-246x.2010.04896.x

Bauer, A., Reimink, J., Chacko, T., Foley, B. J., Shirey, S., & Pearson, D. (2020). Hafnium isotopes in zircons document the gradual onset of mobile-lid tectonics. Geochemical Perspectives Letters, 14, 1–6. https://doi.org/10.7185/geochemlet.2015

Bédard, J. H. (2018). Stagnant lids and mantle overturns: Implications for Archaean tectonics, magmagenesis, crustal growth, mantle evolution, and the start of plate tectonics. Geoscience Frontiers, 9(1), 19–49. https://doi.org/10.1016/j.gsf.2017.01.005

and the start of plate tectonics. Geoscience Frontiers, 9(1), 19–49. https://doi.org/10.1016/j.gst.2017.01.005

Bercovici, D., Mulyukova, E., Girard, J., & Skemer, P. (2023). A coupled model for phase mixing, grain damage and shear localization in the lithosphere: Comparison to lab experiments. Geophysical Journal International, 232(3), 2205–2230. https://doi.org/10.1093/gji/ggac428

Bercovici, D., & Ricard, Y. (2012). Mechanisms for the generation of plate tectonics by two-phase grain-damage and pinning. *Physics of the Earth and Planetary Interiors*, 202, 27–55. https://doi.org/10.1016/j.pepi.2012.05.003

CHOI AND FOLEY 22 of 25

21699356, 2024, 10, Downloaded from https:

Journal of Geophysical Research: Solid Earth

- Bercovici, D., & Ricard, Y. (2013). Generation of plate tectonics with two-phase grain-damage and pinning: Source–sink model and toroidal flow. Earth and Planetary Science Letters, 365, 275–288. https://doi.org/10.1016/j.epsl.2013.02.002
- Bercovici, D., Ricard, Y., & Schubert, G. (2001). A two-phase model for compaction and damage: 1. General theory. *Journal of Geophysical Research*, 106(B5), 8887–8906. https://doi.org/10.1029/2000jb900430
- Beuchert, M. J., & Podladchikov, Y. Y. (2010). Viscoelastic mantle convection and lithospheric stresses. *Geophysical Journal International*, 183(1), 35–63. https://doi.org/10.1111/j.1365-246x.2010.04708.x
- Bowring, S. A., & Williams, I. S. (1999). Priscoan (4.00–4.03 ga) orthogneisses from northwestern Canada. Contributions to Mineralogy and Petrology, 134(1), 3–16. https://doi.org/10.1007/s004100050465
- Boyd, F., & Gurney, J. J. (1986). Diamonds and the African lithosphere. Science, 232(4749), 472–477. https://doi.org/10.1126/science.232 4749.472
- Brace, W., & Kohlstedt, D. (1980). Limits on lithospheric stress imposed by laboratory experiments. *Journal of Geophysical Research*, 85(B11), 6248–6252. https://doi.org/10.1029/ib085ib11p06248
- Brown, M. (2006). Duality of thermal regimes is the distinctive characteristic of plate tectonics since the Neoarchean. *Geology*, 34(11), 961–964. https://doi.org/10.1130/g22853a.1
- Byerlee, J. (1978). Friction of rocks. In Rock friction and earthquake prediction (pp. 615-626). Springer.
- Cawood, P. A., Kroner, A., & Pisarevsky, S. (2006). Precambrian plate tectonics: Criteria and evidence. *Geological Society of America Today*, 16(7), 4. https://doi.org/10.1130/gsat01607.1
- Christensen, N. I., & Mooney, W. D. (1995). Seismic velocity structure and composition of the continental crust: A global view. *Journal of Geophysical Research*, 100(B6), 9761–9788. https://doi.org/10.1029/95jb00259
- Condie, K. C., & Kröner, A. (2008). When did plate tectonics begin? Evidence from the geologic record. In *When did plate tectonics begin on planet Earth* (Vol. 440, pp. 281–294). Geological Society of America Special Papers, https://doi.org/10.1130/2008.2440(14)
- Cross, A., & Skemer, P. (2019). Rates of dynamic recrystallization in geologic materials. *Journal of Geophysical Research: Solid Earth*, 124(2), 1324–1342. https://doi.org/10.1029/2018jb016201
- De Bresser, J., Ter Heege, J., & Spiers, C. (2001). Grain size reduction by dynamic recrystallization: Can it result in major rheological weakening? International Journal of Earth Sciences, 90(1), 28–45. https://doi.org/10.1007/s005310000149
- Dick, G. J. (2019). The microbiomes of deep-sea hydrothermal vents: Distributed globally, shaped locally. *Nature Reviews Microbiology*, 17(5), 271–283. https://doi.org/10.1038/s41579-019-0160-2
- Evans, B., Renner, J., & Hirth, G. (2001). A few remarks on the kinetics of static grain growth in rocks. *International Journal of Earth Sciences*, 90(1), 88–103. https://doi.org/10.1007/s005310000150
- Fei, H., Koizumi, S., Sakamoto, N., Hashiguchi, M., Yurimoto, H., Marquardt, K., et al. (2016). New constraints on upper mantle creep mechanism inferred from silicon grain-boundary diffusion rates. Earth and Planetary Science Letters, 433, 350–359. https://doi.org/10.1016/j. epsl 2015 11 014
- Finnerty, A. (1987). Thermobarometry for garnet peridotites: Basis for the determination of thermal and compositional structure of the upper mantle. *Mantle Xenolith*, 403–412.
- Foley, B. J. (2015). The role of plate tectonic–climate coupling and exposed land area in the development of habitable climates on rocky planets. The Astrophysical Journal, 812(1), 36. https://doi.org/10.1088/0004-637x/812/1/36
- Foley, B. J. (2018a). On the dynamics of coupled grain size evolution and shear heating in lithospheric shear zones. *Physics of the Earth and Planetary Interiors*, 283, 7–25. https://doi.org/10.1016/j.pepi.2018.07.008
- Foley, B. J. (2018b). The dependence of planetary tectonics on mantle thermal state: Applications to early earth evolution. *Philosophical Transactions of the Royal Society A: Mathematical, Physical & Engineering Sciences*, 376(2132), 20170. https://doi.org/10.1098/rsta.2017.0409
- Foley, B. J. (2020). Timescale of short-term subduction episodicity in convection models with grain damage: Applications to Archean tectonics. Journal of Geophysical Research: Solid Earth, 125(12), e2020JB020, https://doi.org/10.1029/2020jb020478
- Foley, B. J., Bercovici, D., & Elkins-Tanton, L. T. (2014). Initiation of plate tectonics from post-magma ocean thermochemical convection. Journal of Geophysical Research: Solid Earth, 119(11), 8538–8561. https://doi.org/10.1002/2014jb011121
- Foley, B. J., & Rizo, H. (2017). Long-term preservation of early formed mantle heterogeneity by mobile lid convection: Importance of grainsize evolution. Earth and Planetary Science Letters, 475, 94–105. https://doi.org/10.1016/j.epsl.2017.07.031
- Griffin, W., O'Reilly, S. Y., Natapov, L., & Ryan, C. (2003). The evolution of lithospheric mantle beneath the Kalahari craton and its margins. Lithos, 71(2–4), 215–241. https://doi.org/10.1016/j.lithos.2003.07.006
- Gurnis, M., Hall, C., & Lavier, L. (2004). Evolving force balance during incipient subduction. *Geochemistry, Geophysics, Geosystems*, 5(7). https://doi.org/10.1029/2003gc000681
- Hall, C. E., Gurnis, M., Sdrolias, M., Lavier, L. L., & Müller, R. D. (2003). Catastrophic initiation of subduction following forced convergence across fracture zones. Earth and Planetary Science Letters, 212(1-2), 15-30. https://doi.org/10.1016/s0012-821x(03)00242-5
- Harrison, T. M. (2009). The Hadean crust: Evidence from> 4 ga zircons. Annual Review of Earth and Planetary Sciences, 37(1), 479–505. https://doi.org/10.1146/annurev.earth.031208.100151
- Hawkesworth, C., O'nions, R., Pankhurst, R., Hamilton, P., & Evensen, N. (1977). A geochemical study of island-arc and back-arc tholeites from the scotia sea. Earth and Planetary Science Letters, 36(2), 253–262. https://doi.org/10.1016/0012-821x(77)90207-2
- Herzberg, C., Condie, K., & Korenaga, J. (2010). Thermal history of the earth and its petrological expression. *Earth and Planetary Science Letters*, 292(1–2), 79–88. https://doi.org/10.1016/j.epsl.2010.01.022
- Hirth, G., & Kohlstedt, D. (2003). Rheology of the upper mantle and the mantle wedge: A view from the experimentalists. *Geophysical Monograph-American Geophysical Union*, 138, 83–106.
- Hopkins, M., Harrison, T. M., & Manning, C. E. (2008). Low heat flow inferred from> 4 gyr zircons suggests Hadean plate boundary interactions. Nature, 456(7221), 493–496. https://doi.org/10.1038/nature07465
- lizuka, T., Horie, K., Komiya, T., Maruyama, S., Hirata, T., Hidaka, H., & Windley, B. F. (2006). 4.2 Ga zircon xenocryst in an Acasta gneiss from northwestern Canada: Evidence for early continental crust. *Geology*, 34(4), 245–248. https://doi.org/10.1130/g22124.1
- James, D., Fouch, M., VanDecar, J., Van Der Lee, S., & Group, K. S. (2001). Tectospheric structure beneath southern Africa. Geophysical Research Letters, 28(13), 2485–2488. https://doi.org/10.1029/2000gl012578
- Kasting, J. F., & Catling, D. (2003). Evolution of a habitable planet. Annual Review of Astronomy and Astrophysics, 41(1), 429–463. https://doi.org/10.1146/annurev.astro.41.071601.170049
- Kemp, A. I. S. (2018). Early Earth geodynamics: Cross examining the geological testimony. Philosophical Transactions of the Royal Society A: Mathematical, Physical & Engineering Sciences, 376(2132), 20180169. https://doi.org/10.1098/rsta.2018.0169

CHOI AND FOLEY 23 of 25



Journal of Geophysical Research: Solid Earth

- 10.1029/2024JB029136
- Korenaga, J. (2013). Initiation and evolution of plate tectonics on earth: Theories and observations. *Annual Review of Earth and Planetary Sciences*, 41(1), 117–151. https://doi.org/10.1146/annurev-earth-050212-124208
- Lenardic, A. (1997). On the heat flow variation from Archean cratons to proterozoic mobile belts. *Journal of Geophysical Research*, 102(B1), 709–721. https://doi.org/10.1029/96jb02849
- Lenardic, A., & Moresi, L.-N. (1999). Some thoughts on the stability of cratonic lithosphere: Effects of buoyancy and viscosity. *Journal of Geophysical Research*, 104(B6), 12747–12758. https://doi.org/10.1029/1999jb900035
- Lenardic, A., Moresi, L.-N., & Mühlhaus, H. (2003). Longevity and stability of cratonic lithosphere: Insights from numerical simulations of coupled mantle convection and continental tectonics. *Journal of Geophysical Research*, 108(B6). https://doi.org/10.1029/2002jb001859
- Maher, K., & Chamberlain, C. (2014). Hydrologic regulation of chemical weathering and the geologic carbon cycle. *Science*, 343(6178), 1502–1504. https://doi.org/10.1126/science.1250770
- Manga, M., & O'Connell, R. J. (1995). The tectosphere and postglacial rebound. Geophysical Research Letters, 22(15), 1949–1952. https://doi.org/10.1029/95gl02012
- Martin, W., Baross, J., Kelley, D., & Russell, M. J. (2008). Hydrothermal vents and the origin of life. *Nature Reviews Microbiology*, 6(11), 805–814. https://doi.org/10.1038/nrmicro1991
- McKenzie, D. (1977). The initiation of trenches: A finite amplitude instability. In *Island arcs, deep sea trenches and back-arc basins* (Vol. 1, pp. 57–61). https://doi.org/10.1029/me001p0057
- Michaut, C., Jaupart, C., & Bell, D. (2007). Transient geotherms in archean continental lithosphere: New constraints on thickness and heat production of the subcontinental lithospheric mantle. *Journal of Geophysical Research*, 112(B4). https://doi.org/10.1029/2006jb004464
- Moore, W. B., & Webb, A. A. G. (2013). Heat-pipe earth. *Nature*, 501(7468), 501–505. https://doi.org/10.1038/nature12473

 Moresi, L., & Solomatov, V. (1998). Mantle convection with a brittle lithosphere: Thoughts on the global tectonic styles of the Earth and Venus.
- Geophysical Journal International, 133(3), 669–682. https://doi.org/10.1046/j.1365-246x.1998.00521.x Mulyukova, E., & Bercovici, D. (2017). Formation of lithospheric shear zones: Effect of temperature on two-phase grain damage. Physics of the
- Earth and Planetary Interiors, 270, 195–212. https://doi.org/10.1016/j.pepi.2017.07.011
 O'Neill, C., Debaille, V., & Griffin, W. (2013). Deep earth recycling in the Hadean and constraints on surface tectonics. American Journal of
- Science, 313(9), 912–932. https://doi.org/10.2475/09.2013.04
 Palin, R. M., Santosh, M., Cao, W., Li, S.-S., Hernández-Uribe, D., & Parsons, A. (2020). Secular change and the onset of plate tectonics on Earth.
- Earth-Science Reviews, 207(103), 172. https://doi.org/10.1016/j.earscirev.2020.103172

 Parnell, J. (2004). Plate tectonics, surface mineralogy, and the early evolution of life. International Journal of Astrobiology, 3(2), 131–137. https://
- Parnell, J. (2004). Plate tectonics, surface mineralogy, and the early evolution of life. *International Journal of Astrobiology*, 3(2), 131–137. https://doi.org/10.1017/S1473550404002101
- Patočka, V., Čížková, H., & Tackley, P. (2019). Do elasticity and a free surface affect lithospheric stresses caused by upper-mantle convection? Geophysical Journal International, 216(3), 1740–1760. https://doi.org/10.1093/gji/ggy513
- Pollack, H. N. (1986). Cratonization and thermal evolution of the mantle. Earth and Planetary Science Letters, 80(1–2), 175–182. https://doi.org/10.1016/0012-821x(86)90031-2
- Reimink, J., Pearson, D., Shirey, S., Carlson, R., & Ketchum, J. (2019). Onset of new, progressive crustal growth in the central slave craton at 3.55 ga. *Geochemical Perspective Letters*, 10, 8–13. https://doi.org/10.7185/geochemlet.1907
- Reimink, J. R., Chacko, T., Stern, R. A., & Heaman, L. M. (2014). Earth's earliest evolved crust generated in an iceland-like setting. *Nature Geoscience*, 7(7), 529–533. https://doi.org/10.1038/ngeo2170
- Reimink, J. R., Chacko, T., Stern, R. A., & Heaman, L. M. (2016). The birth of a cratonic nucleus: Lithogeochemical evolution of the 4.02–2.94 ga Acasta gneiss complex. *Precambrian Research*, 281, 453–472. https://doi.org/10.1016/j.precamres.2016.06.007
- Rey, P. F., Coltice, N., & Flament, N. (2014). Spreading continents kick-started plate tectonics. *Nature*, 513(7518), 405–408. https://doi.org/10.1038/nature13728
- Rolf, T., & Tackley, P. (2011). Focussing of stress by continents in 3D spherical mantle convection with self-consistent plate tectonics. Geophysical Research Letters, 38(18), https://doi.org/10.1029/2011gl048677
- Rozel, A., Ricard, Y., & Bercovici, D. (2011). A thermodynamically self-consistent damage equation for grain size evolution during dynamic recrystallization. Geophysical Journal International, 184(2), 719–728. https://doi.org/10.1111/j.1365-246x.2010.04875.x
- Santosh, M., Arai, T., & Maruyama, S. (2017). Hadean earth and primordial continents: The cradle of prebiotic life. *Geoscience Frontiers*, 8(2), 309–327. https://doi.org/10.1016/j.gsf.2016.07.005
- Skemer, P., & Karato, S.-i. (2008). Sheared Iherzolite xenoliths revisited. Journal of Geophysical Research, 113(B7). https://doi.org/10.1029/2007jb005286
- Solomatov, V. (2004). Initiation of subduction by small-scale convection. *Journal of Geophysical Research*, 109(B1). https://doi.org/10.1029/
- Speciale, P., Behr, W. M., Hirth, G., & Tokle, L. (2020). Rates of olivine grain growth during dynamic recrystallization and postdeformation annealing. *Journal of Geophysical Research: Solid Earth*, 125(11), e2020JB020. https://doi.org/10.1029/2020jb020415
- Steinberger, B., & Becker, T. W. (2018). A comparison of lithospheric thickness models. *Tectonophysics*, 746, 325–338. https://doi.org/10.1016/j.tecto.2016.08.001
- Stern, R. J. (2005). Evidence from ophiolites, blueschists, and ultrahigh-pressure metamorphic terranes that the modern episode of subduction tectonics began in neoproterozoic time. Geology, 33(7), 557–560. https://doi.org/10.1130/g21365.1
- Stern, R. J., & Gerya, T. (2018). Subduction initiation in nature and models: A review. Tectonophysics, 746, 173–198. https://doi.org/10.1016/j.tecto.2017.10.014
- Tackley, P. J. (2000a). Self-consistent generation of tectonic plates in time-dependent, three-dimensional mantle convection simulations 2. strain weakening and asthenosphere. *Geochemistry, Geophysics, Geosystems*, 1(8). https://doi.org/10.1029/2000gc000043
- Tackley, P. J. (2000b). Self-consistent generation of tectonic plates in time-dependent, three-dimensional mantle convection simulations. Geochemistry, Geophysics, Geosystems, 1(8). https://doi.org/10.1029/2000gc000036
- Tang, M., Chen, K., & Rudnick, R. L. (2016). Archean upper crust transition from mafic to felsic marks the onset of plate tectonics. *Science*, 351(6271), 372–375. https://doi.org/10.1126/science.aad5513
- Tasaka, M., Zimmerman, M. E., Kohlstedt, D. L., Stünitz, H., & Heilbronner, R. (2017). Rheological weakening of olivine+ orthopyroxene aggregates due to phase mixing: Part 2. Microstructural development. *Journal of Geophysical Research: Solid Earth*, 122(10), 7597–7612. https://doi.org/10.1002/2017jb014311
- Taylor, S. R., & McLennan, S. (1981). The composition and evolution of the continental crust: Rare earth element evidence from sedimentary rocks. Philosophical Transactions of the Royal Society of London Series A: Mathematical and Physical Sciences, 301(1461), 381–399.
- Toth, J., & Gurnis, M. (1998). Dynamics of subduction initiation at preexisting fault zones. *Journal of Geophysical Research*, 103(B8), 18053–18067. https://doi.org/10.1029/98jb01076

CHOI AND FOLEY 24 of 25



Journal of Geophysical Research: Solid Earth

- 10.1029/2024JB029136
- Ulvrova, M. M., Coltice, N., Williams, S., & Tackley, P. J. (2019). Where does subduction initiate and cease? A global scale perspective. *Earth and Planetary Science Letters*, 528(115), 836. https://doi.org/10.1016/j.epsl.2019.115836
- Van Heck, H., & Tackley, P. (2008). Planforms of self-consistently generated plates in 3D spherical geometry. *Geophysical Research Letters*, 35(19). https://doi.org/10.1029/2008gl035190
- Van Kranendonk, M. J. (2011). Onset of plate tectonics. Science, 333(6041), 413-414. https://doi.org/10.1126/science.1208766
- Van Kranendonk, M. J., Smithies, R. H., Griffin, W. L., Huston, D. L., Hickman, A. H., Champion, D. C., et al. (2015). Making it thick: A volcanic plateau origin of palaeoarchean continental lithosphere of the Pilbara and Kaapvaal cratons. *Geological Society, London, Special Publications*, 389(1), 83–111. https://doi.org/10.1144/sp389.12
- Wang, H., van Hunen, J., & Pearson, D. G. (2018). Making Archean cratonic roots by lateral compression: A two-stage thickening and stabilization model. *Tectonophysics*, 746, 562–571. https://doi.org/10.1016/j.tecto.2016.12.001
- Warren, J. M., & Hirth, G. (2006). Grain size sensitive deformation mechanisms in naturally deformed peridotites. *Earth and Planetary Science Letters*, 248(1–2), 438–450. https://doi.org/10.1016/j.epsl.2006.06.006
- Weller, M., & Lenardic, A. (2012). Hysteresis in mantle convection: Plate tectonics systems. Geophysical Research Letters, 39(10). https://doi.org/10.1029/2012gl051232
- Wiesman, H. S., Zimmerman, M. E., & Kohlstedt, D. L. (2018). Laboratory investigation of mechanisms for phase mixing in olivine+ ferro-periclase aggregates. Philosophical Transactions of the Royal Society A: Mathematical, Physical & Engineering Sciences, 376(2132), 20170–20417. https://doi.org/10.1098/rsta.2017.0417
- Zhou, X., & Wada, I. (2022). Effects of elasticity on subduction initiation: Insight from 2-d thermomechanical models. *Journal of Geophysical Research: Solid Earth*, 127(11), e2022JB024. https://doi.org/10.1029/2022jb024400

CHOI AND FOLEY 25 of 25